DEPARTMENT OF THE NAVY

HYDROMECHANICS

○

AERODYNAMICS

○

STRUCTURAL
MECHANICS

○

APPLIED
MATHEMATICS

○

ACOUSTICS AND
VIBRATION

WAKE ANALYSIS OF A SERIES 60,

0.60 BLOCK COEFFICIENT MODEL,

MODEL 4210-5

by

J. B. Hadler

and
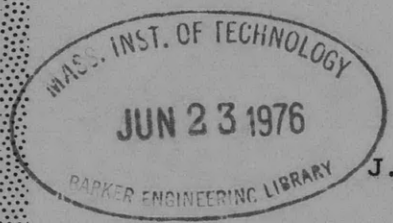
A. H. Weaver

RESEARCH AND DEVELOPMENT REPORT

October 1965

Report 2075

WAKE ANALYSIS OF A SERIES 60,

0.60 BLOCK COEFFICIENT MODEL,

MODEL 4210-5

by

J. B. Hadler

and

A. H. Weaver

TABLE OF CONTENTS

LIST OF FIGURES

LIST OF FIGURES (Continued)

Page

Page

D	Propeller diameter
J_a	Apparent advance coefficient V/nD
n	Propeller revolutions
P	Pressure factor $(V_b^2)_{max} / \overline{V_b^2} - 1$.
R	Radius of propeller
r	Radial coordinate
U	Blade element velocity
V	Model or ship velocity
$\underline{V}$	Resultant wake velocity vector
V_b	Resultant inflow velocity to blade
$\overline{V}_b$	Mean resultant inflow velocity to blade
V_r	Radial component of velocity vector
$\overline{V}_r$	Mean radial component of velocity vector
V_t	Tangential component of velocity vector
$\overline{V}_t$	Mean tangential component of velocity vector
$(\tilde{V}_t)_n$	n^{th} harmonic amplitude of tangential velocity
V_{tr}	Transverse component of velocity vector
$\overline{V}_v$	Volumetric velocity
V_x	Longitudinal component of velocity vector (normal to the plane of propeller)
$\overline{V}_x$	Mean longitudinal component of velocity vector
$(\tilde{V}_x)_n$	n^{th} harmonic amplitude of longitudinal velocity

W_x Volumetric mean wake velocity

X, Y, Z   Cartesian coordinates

α_h Projected angle of velocity vector on X-Y plane

α_v Projected angle of velocity vector on X-Z plane

β Advance angle in degree

$\bar{\beta}$ Mean advance angle

$\Delta\beta$ Variation of advance angle from its mean

θ Position angle (angular coordinate) in degrees

Hull coefficients are in accordance with SNAME recommended standard.

ABSTRACT

This report presents the results of the wake analysis
of a single-screw Series 60 model having a block coeffi-
cient of 0.60. The data presented include the interpolated
longitudinal and tangential velocity distributions, and the
effect on wake harmonics due to variations in speed, longi-
tudinal position of rudder and plane of survey, draft, and
trim.

ADMINISTRATIVE INFORMATION

INTRODUCTION

The David Taylor Model Basin, through the General Hydromechanics
Research Program, has undertaken an extensive program of analyzing
wake surveys made on surface ship models tested over the past twenty
years. The objective of this work is to analyze the wake data as a
whole, and to provide guidance to the ship and propeller designers in
achieving better overall propeller-ship forms. Since most of these
wake surveys have been performed on individual ship designs, it is
difficult to make comparisons until the effects of speed, propeller
and rudder position, displacement, trim, and the repeatability of test
data are known upon the wake pattern. With this problem in mind, an
auxiliary program was established to investigate these problems before
the analysis of the existing wake surveys was completed. Since the
answers to these questions are more uncertain on ships where the
propeller operates in the viscous boundary layer of the hull, it was
decided to undertake the experiments on the high-speed cargo, or

replenishment-type ship. Most of the existing wake survey data are for this type of ship.

The method of analysis employed in this report is the same as that used in the material already published on the single-screw DE, Reference 1, and the twin-screw DD, Reference 2. The data presented are the radial distribution of the mean longitudinal velocity, the volumetric mean velocity, the amplitude of the longitudinal and tangential harmonics, and finally the angular and velocity variations of the resultant velocity to the propeller blade elements.

TEST PROCEDURE

This series of experiments was conducted with Model 4210-5. The hull is constructed of wax and is the parent Series 60, 0.60 C_B model with the stern altered to the "clearwater" type which is more representative of current ship building practice than the type used on the original Series 60. Model dimensions and coefficients, sectional area curves, and the abbreviated lines for this hull are presented in Figure 1. Also included in Figure 1 is a tabulation of some of the major dimensions for 400-ft and 600-ft LBP ships.

The measurements were made with a 5-hole pitot tube which has a $\frac{1}{2}$-in.-diameter spherical head (designated as Tube 3A). The instrumentation was installed in accordance with standard Model Basin practice, which is described in Reference 3.

The pitot-tube assembly base plate was mounted on the stern of the model parallel to the propeller shaft. After the horizontal and transverse slides and the pitot tube were each fitted into place, a flexible tube from each of the five orifices in the head of the pitot tube was connected to a straight tube of a water manometer board. A sixth tube of the manometer board was connected to an open-top container of water located near the water surface of the test basin and

used for static readings. A vacuum is applied through two tanks to a
manifold located at the top of the manometer board, and the height of
the water is pulled to a convenient reading level which is approxi-
mately 60 in. above the water level of the test basin. A schematic
of the pressure system is presented as Figure 2.

The model test program is outlined in the table below.

TEST NUMBER	POSITION FOR PLANE OF SURVEY	RUDDER POSITION	MODEL SPEED knots	DISPLACEMENT pounds	TRIM BY STERN feet
1	1	None	4.38	1489	0.48
2	1	None	3.90	2127	0
3P (port side)	1	None	4.38	2127	0
3S (stbd side)	1	None	4.38	2127	0
3PR (repeat of port side)	1	None	4.38	2127	0
4	1	None	5.10	2127	0
5	1	B	4.38	2127	0
6	1	A	4.38	2127	0
7	2	None	4.38	2127	0
8	1	None	4.38	1276	0.48

The longitudinal positions for the plane of survey noted in the
table are defined as Positions 1 and 2 and are measured from the stern
frame to the centerline of the propeller at the 0.7 radius at the
0-deg position. The rudder positions are expressed as Positions A
and B and are measured from the stern frame to the leading edge of
the rudder at the 0.7 propeller radius. A sketch showing these
locations in model dimensions is presented as Figure 3.

The basic test (Test 3P) was with the hull ballasted to the design (100 percent) displacement condition, even keel, the plane of survey at Position 1 without rudder, and at the model speed of 4.38 knots. Measurements were made on the port (Test 3P) and starboard (Test 3S) sides at the 0.40, 0.70, and 0.95 radii at 15 angular positions each. A vector diagram showing the location where the measurements were made is presented as Figure 4. The coordinate system of the velocity components is explained in Figure 5.

Tests 3P, 2, 4, 5, 6, and 7 were conducted simultaneously. When measurements were being made at the angular positions of 0, 5, 10, 15, 20, 40, 90, 150, 165, 170, 175, and 180 deg for the basic test 3P, Tests 2, 4, 5, and 6 were accomplished without changing the location of the pitot tube. This meant for Tests 2 and 4 a change in model speed and for Tests 5 and 6 the introduction of the rudder which was designed to be easily mountable under water. After all of the above tests had been completed at Position 1, the rudder was then removed and the pitot tube moved forward to Position 2 for Test 7. This method of testing maintained the same relative position in the transverse plane and insured the greatest accuracy possible. For Tests 3P and 7, measurements were also made at 30, 60, 120, and 160 deg.

In order to position the rudder when the pitot tube was near the centerline, it was necessary to cut away a section of the rudder at various vertical positions. This was accomplished by constructing six rudders — each with a section cut away at a height to accommodate the tube at a specific percent of the propeller radius. Photographs of the various rudders and rudder and tube locations are presented as Figures 6, 7, and 8.

After completion of the above experiments, the model was re-ballasted to 60 percent of the design displacement and trimmed in such a manner that the propeller tip below surface was the same as if the model was at 80 percent displacement, even keel. Measurements for Test 8 were taken at the same 36 locations as in Tests 2, 4, 5, and 6.

Subsequently, it was found that the 60-percent displacement con-
dition was too light for vibration experiments which were also being
conducted on this model, so a further test, designated Test 1, was
conducted in which the same trim was maintained but the displacement
was increased to 70 percent of that of the design displacement. In
order that the data could be directly usable in the vibration work,
the wake measurements were made in the forward position, Position 2.

Finally, when preliminary analysis of the data revealed unsus-
pectedly large differences between Tests 3P and 3S, it was decided to
conduct a repeat test on the port side, Test 3PR.

All of the data from these experiments have been analyzed by
the computer program described in Reference 4.

PRESENTATION OF DATA

Two types of information are presented in this report: the test
data and the computed results. The test data are those obtained from
the model experiments at the prescribed test points. The computed
data are the quantities calculated on the basis of the test data.
The data are nondimensionalized, based on a 400-ft and a 600-ft LBP
ship with propeller diameters of 16.6 and 24.9 ft, respectively.

Figures 9 through 14 show the interpolated circumferential dis-
tribution of the longitudinal and tangential velocity components at
the test radii. Each of the three test radii shows the typical velocity
distribution experienced on the cargo-type ship with clearwater stern.
The 0.40 r/R shows a fairly symmetrical type of distribution with the
velocity defect at the lower part of the hull approaching that for the
upper part of the hull. The 0.70 r/R shows a very narrow region of
reduced velocity due to the influence of the lower part of the hull
and the 0.95 r/R shows no velocity defect in the lower part of the hull.

These circumferential distribution curves of both the longitudi-
nal and tangential velocities are analyzed for their harmonic contents.

The radial distribution of the mean longitudinal velocity $\bar{V}_x/V$, obtained from the harmonic analysis, is shown in Figures 15 through 20. These figures also show the calculated volumetric velocity and its mean value for the various tests; their definitions are given in Reference 1.

The amplitude and phase angles of various orders of harmonics are obtained from the harmonic analysis of the velocity curves. Figures 22 through 27 show the amplitude and phase angle for the longitudinal component for the harmonics of orders up to 8. Figures 28 through 33 show the same for the tangential component. In general, as shown in Figure 21, these harmonics show a decrease in amplitude with increase in order. The even orders tend to be stronger than the odd orders.

For the purposes of furnishing useful information in analyzing the cavitation characteristics of a propeller operating in a nonuniform wake field, the wake data have been further analyzed in terms of the maximum resultant velocities to the propeller blade and the fluctuations in the advance angle. As can be readily shown, the velocity at the blade element depends upon the propeller rotational speed. In order to establish proper geometric relationships, it is necessary to assume certain operating conditions, namely, the advance coefficient J_a. A value of 0.922 was chosen for this analysis. Figures 34 through 39 show the calculated values of the maximum variations $\pm \Delta \beta$ from the mean advance angle. This means that the fluctuation of the advance angle may be anywhere within the boundaries of $+ \Delta \beta$ and $- \Delta \beta$ curves.

The primary factor in determining the magnitude of the $- \Delta \beta$ quantity is the longitudinal velocity defect in the region immediately behind the hull centerline. Special care was taken in these experiments to get as many measurements in that region as practical because of the known high velocity gradient and the general instability of the flow in this region. Also shown on the same figures are the so-called pressure factors, which represent the minimum pressures of the propeller blade element resulting from the fluctuations in the inflow velocity expressed as a percent of the mean resultant velocity at that particular blade element.

DISCUSSION

In comparing the results of this series of experiments, each item investigated will be taken up separately after a brief discussion on the accuracy of the pitot-tube manometer system of measurement. The investigation of the effect of rudder will be taken up first, followed by the effect of speed. These two tests provide the most precise comparisons and establish the best accuracy possible with the current measuring system. The experiments on symmetry and repeatability, effect of plane of measurement, and effect of trim and displacement follow. All comparisons are made with the basic test (3P).

ACCURACY OF MEASUREMENT

Since these experiments involved comparisons of velocity measurements on the same model, the first step is an evaluation of the accuracy of the pitot-tube manometer system of measurement. Appendix A describes the procedure used to evaluate both the 5-hole pitot tube used for the experiments contained in this report and its predecessor, the 1-in.-diameter 13-hole pitot tube.

Based on the results from the $\frac{1}{2}$-in. pitot tube, these experiments show that at speeds of 3, 2, 1.5, and 1 knots, the maximum error in speed is 1, 2, 4, and 9 percent, respectively. The minimum velocity measured on most of these experiments was about 1.5 knots, with two of the experiments (Tests 1 and 7) showing centerplane velocities as low as 0.9 of a knot. The maximum probable error in speed is about 4 and 11 percent, respectively, which corresponds to 1.4 and 2.3 percent for the model speed of 4.38 knots.

EFFECT OF RUDDER (TESTS 3P, 5, AND 6)

In this set of experiments, the rudder was introduced at two different positions in relation to the plane of measurement, as shown in Figures 3, 6, and 7. To insure the greatest accuracy possible,

the pitot tube was retained in a fixed position, and the rudder introduced and moved forward before going to the next test spot. This insured no movement of the pitot tube or change in angular position.

These experiments, the results of which are shown in Figures 12, 18, 25, 31, and 37, are the most consistent of the whole series. The effect of the rudder is apparent only at the top of the propeller disk where the velocity defect is increased between 4 and 6 points (4 and 6 percent of model speed). The scatter shown in the region from about 20 deg to about 90 deg in the inner radii is believed due to the rotational, thus less stable, nature of the flow. The rotational character of the velocity field can be observed in Figure 4.

Figures 25 and 31 compare the amplitude and phase of the harmonics. Within the experimental limitations already discussed, the results appear consistent. No significant effect on the harmonics can be expected from the introduction of the rudder. .

The values of + $\Delta\beta$ and pressure coefficients are very consistent, as shown in Figure 37. The variations are less than ½ deg. The - $\Delta\beta$ shows a variation as great as 1 deg between the conditions with and without the rudder. This, of course, is due to the increased velocity defect noted at the top of the propeller disk. In general, it can be concluded that it is not necessary to have the rudder in place when conducting wake surveys, although it should be recognized that the value of - $\Delta\beta$ may be slightly larger in the presence of the rudder.

EFFECT OF SPEED (TESTS 3P, 2, AND 4)

This experiment consisted of making velocity measurements at three speeds; thus comparisons of the effect of speed are possible over a range of speed length-ratios from 0.87 to 1.13. As indicated previously, the pitot-tube position was fixed for each spot and the speed varied.

Comparable accuracy to the tests with and without the rudder

just described would be expected. The results are shown in Figures 10, 16, 23, 29, and 35.

The circumferential plots, Figure 10, of the two velocity components show only a slightly larger variation than those obtained on the rudder tests in Figure 12. This would indicate there is some effect from speed, but the differences shown are largely masked by the flow instability just discussed. If there is any effect from speed, it would probably arise from the change in location of the wave train and the effect it has on the longitudinal velocity profile over the propeller disk. This effect should be most pronounced on the first harmonic. This appears to be indicated in Figures 23 and 29. The shapes of the third, fourth, and fifth harmonics of the longitudinal velocity component are altered. It is possible that this is largely the result of the fairing techniques since only three radii were measured. In future experiments with more refined techniques and with more test spots, this doubt will be eliminated.

The effect of speed upon the advance angle β and inflow velocity is discernable. The greatest change occurs in the $-\triangle\beta$ quantity since it is dominated by the changes in velocity which occur at the centerplane of the model.

SYMMETRY AND REPEATABILITY (TESTS 3P, 3S, AND 3PR)

This experiment consisted of measuring the port, 3P, and starboard side, 3S, of the model, and then at a later time, remeasuring the port side, 3PR, at the same angular positions. On ship models of this type, measurements are made over only one-half of the propeller plane, usually the port side, and symmetry assumed. It was the objective of this test to determine if this assumption was reasonable as there has been evidence from wind tunnel tests on submarine models that this is not always true (Reference 6). The objective of the repeat test was to obtain direct evidence of the consistency of test results since submarine models had shown surprising variations.

9

The results are shown in Figures 11, 17, 24, 30, and 36. Figure 11 indicates that the scatter between tests is disconcertingly large. The variations are not confined to a particular region of the disk and are as much as 10 percent of the ship speed, even in regions where there is a small velocity gradient, nor do they appear to be particularly confined to either the starboard side or to the repeat measurements. The comparison of the mean longitudinal velocity $\overline{V}_x/V$ in Figure 17 shows that the repeat test (3PR) is about 4 points higher than the original test (3P). The starboard test (3S) agrees with Test 3P at the inner radii, but with Test 3PR at the outer radii. The two port side tests have been thoroughly checked for any consistent error, but none has been found. The comparison of the harmonics, Figures 24 and 30, seems to show slightly better agreement between the two port side measurements for most of the harmonics, but the scatter of results is too great.

The variations in the $\pm \Delta \beta$ and P values are shown in Figure 36. The variations are within about 1 deg for both the $- \Delta \beta$ and the $+ \Delta \beta$ values.

These experiments rather clearly indicate (1) that any comparisons made between wake patterns on single-screw ship hulls tested in the past must be carefully judged and (2) that the importance of flow instabilities must be determined through improved test equipment and techniques if accurate information is to be derived from wake surveys.

PLANE OF MEASUREMENT (TESTS 3P AND 7)

The purpose of this experiment was to determine the significance of longitudinal position in the aperture. To insure the greatest accuracy practical, these two tests were conducted concurrently by measuring the velocity at each spot in the propeller disk, first in the after position and then in the forward position. The plane of measurement is shown in Figure 3. The results of the experiment are shown in Figures 13, 19, 26, 32, and 38.

As can be seen in Figure 13, the variation is less than that

shown in the repeat tests in Figure 10 except for the region at the top
centerline of the disk where the values have decreased substantially
(7 to 16 points) in the forward position. Surprisingly, the mean longitudinal velocity is about 4 points higher in the forward position, as
shown in Figure 19. This is contrary to other experience at the Model
Basin where the mean velocity decreases as the measurements are taken
closer to the hull (Reference 5). The reason for the increased mean
value is not clear. It cannot be due to moving the pitot tube, nor
can it be due to changes in the flow patterns from one test to the
other since the spots were alternately measured.

This experiment is one of the most interesting in the whole series
for its effect upon the longitudinal harmonics. As may be noted in Figure 26, the odd harmonics have had a significant shift in their amplitude values. This is due to the decrease in velocity noted at the top
of the aperture. The effect on the even harmonics falls within the
range of scatter shown on the other tests. The tangential harmonics
do not show any effect.

The effect on the $+\Delta\beta$ is, of course, negligible, but due to the
greater velocity defect occurring at the top of the disk at the forward
position, the value of $-\Delta\beta$ is increased as much as $3\frac{1}{2}$ deg. This
indicates that the after position in the aperture is better from a
cavitation point of view.

TRIM AND DISPLACEMENT (TESTS 3P, 8, AND 1)

The experiments to determine the effect of displacement and trim
were not varied as systematically as they should to determine independently both the effect of displacement and that of trim. They were
designed to assist in the analysis of the vibration project briefly
discussed in Reference 6. In Test 8, both trim and displacement (60
percent of design) have been varied, but the plane of measurement was
the same as the base test (3P). In Test 1, again both trim (same as
Test 8) (70 percent of design) and displacement were varied, as well

as the plane of measurement (forward position). The results of Test 8 are shown in Figures 14, 20, 27, 33, and 39.

The combined effect of trim and displacement is comparatively large, as shown in Figure 14. It results in a change in slope of the longitudinal mean velocity curve, indicating lower mean velocity at the root and greater at the outer tip of the propeller. The effect on the lower harmonics, Figures 27 and 33, is large. The effect on the advance angle is to reduce the $-\Delta\beta$ and increase the $+\Delta\beta$.

The results of Test 1 are compared in Figures 9, 15, 22, 28, and 34. The change in displacement is less in this test than in Test 8, but the plane of measurement has been moved forward; this latter change dominates the results. We know from Test 7 that the greatest effect of location is in the top part of the propeller disk. This is again obvious for this test, as shown in Figure 9, where the velocity at the centerplane was decreased as much as 22 points, whereas in Test 8 the velocity was actually increased due to the change in trim and displacement. The mean longitudinal velocity $\overline{V}_x/V$, Figure 15, shows the same change in slope as did Test 8. From Test 7 we would expect the magnitude of the odd harmonics of the longitudinal velocity to change when compared with Test 8; however, all harmonics have changed in varying amounts. This is probably due as much to the flow variations and experimental error as to the change in displacement between the two tests.

Similar to Test 7, the $-\Delta\beta$ values show a wide variation, over 4 deg, due again to the larger velocity defect at the top of the aperture.

From the above two tests, it is imperative that each of the effects of displacement and trim should be investigated. We would suspect that changes in displacement would show small effects while the changes in trim would show much larger effects, but this must be demonstrated by careful experiments.

12

CONCLUSIONS

1. The most important finding from these experiments is the comparative inconsistency of the test data, either the repeat measurements or the measurements made on the starboard side. The authors believe these variations are due as much to flow asymmetries and flow instabilities arising from secondary flows as to inaccuracies in model construction, model alignment, repeatability of pitot-tube positioning, and other test errors. It was established that the basic accuracy (open water) of the velocity measuring ($\frac{1}{2}$-in. 5-hole pitot-tube manometer) system was sufficient to contribute little to the inconsistencies noted.

2. Of all the effects studied on this model, by far the most significant is that of propeller position in the aperture. The clearance of the propeller from the stern frame determines the magnitude of the velocities at the centerplane. These values dominate the maximum values of the advance angle and have a significant effect on the amplitude of the wake harmonics, particularly the odd harmonics.

3. It is not necessary to have the rudder in place when conducting wake surveys, although it should be recognized that the rudder may have a small effect on the mean longitudinal velocity and the maximum advance angle.

4. The effect of changes in speed upon the wake patterns appears to be small, but the results in this study are somewhat inconclusive due to the uncertainties in repeat test results.

5. The effect of change in trim and displacement may result in large variations in the wake pattern and, consequently, in the cavitation and vibration characteristics.

6. Any comparisons made between wake patterns on single-screw ship hulls tested in the past must be carefully judged in light of the conclusions above.

RECOMMENDATIONS

1. For the type of study made in this report, instrumentation must be improved, both in accuracy and in speed of acquisition and processing of data.

2. When suitable instrumentation is developed, the study of flow asymmetries and repeatability of measurements should be undertaken.

3. To properly delineate the velocity distribution on the single-screw ship with conventional-type sterns, measurements should be made at four or more radii because of the large variations in the radial direction.

4. A study should be made to investigate the effect of trim.

5. On ship designs which are to operate a significant proportion of time in the ballast condition, it would be well to examine the wake pattern in this condition for the effect it might have upon the propeller design.

6. The effect of speed upon the wake pattern was largely masked by flow instabilities and test inaccuracies; however, it appears to be of sufficient magnitude to warrant further investigation when the test technique is improved.

REFERENCES

1. Cheng, H.M. and Hadler, J.B., "Wake Analysis of Ship Models, Single-Screw DE-Type," David Taylor Model Basin Report 1849 (Jun 1964).

2. Cheng, H.M. and Hadler, J.B., "Wake Analysis of Ship Models, Twin-Screw Military Types," David Taylor Model Basin Report 1928 (Dec 1964).

3. Pien, P.C., "Five-Hole Spherical Pitot Tube," David Taylor Model Basin Report 1229 (May 1958).

4. Cheng, H.M., "Analysis of Wake Survey of Ship Model, Computer Program AML Problem No. 840-219F," David Taylor Model Basin Report 1804 (Mar 1964).

5. Beveridge, J.L., "Effect of Axial Position of Propeller on the Propulsion Characteristics of a Submerged Body of Revolution," David Taylor Model Basin Report 1456 (Mar 1963).

6. Hadler, J.B., "Experimental Determination of Propeller Unsteady Forces at DTMB," Proceedings of the First Conference on Ship Vibration, David Taylor Model Basin Report 2002 (Aug 1965).

ACKNOWLEDGMENTS

15

APPENDIX A

ACCURACY OF PITOT-TUBE MANOMETER MEASURING SYSTEM

The question of accuracy of velocity measurement, particularly in the low velocity region, at the top of the propeller disk of a single-screw ship, frequently arises when detailed analyses are to be made, such as those contained in this report. The question has also been raised of the possibility of laminar flow effects on the $\frac{1}{2}$-in. pitot tube at velocities below 3 ft/sec. To provide an answer to these questions, a set of tests was conducted with the 1-in. 13-hole pitot tube and the $\frac{1}{2}$-in. 5-hole pitot tube and their manometry systems to establish the accuracy. The tests essentially consisted of running the pitot tube into open water, measuring the velocity at 0- and 20-deg yaw angles, and comparing them with the measured carriage speed. The tests were run over a range of speeds from 0.5 to 4.0 knots. The same procedures were used in these tests as were employed in the model wake experiments. The results of these tests plotted with $\Delta H/V^2$ versus V are presented in Figure 42 for the 13- and 5-hole tubes. The scale at the left-hand side of the graph is the difference between H/V^2 as measured by the pitot-tube manometer system and that determined from the calibration; at the right-hand side is a scale for the corresponding error in percent of the speed. Curves shown are the contours for arbitrary errors of $\pm$ 0.025, $\pm$ 0.050, $\pm$ 0.075, and $\pm$ 0.10 in. of water, in manometer board readings (ΔH). From these figures, it is obvious that the 13-hole tube data fall within the test procedure criteria of $\pm$ 0.050 in. of water, and this introduces less than a 2-percent error for speeds greater than $1\frac{1}{2}$ knots. Below this speed, the error increases rapidly, and below 1 knot the error is 5 percent or greater. The results on the $\frac{1}{2}$-in. 5-hole pitot tube are not as accurate, indicating a possible error within the range of $\pm$ 0.10 in. of water. This may be attributed to the fact that this smaller

pitot tube has smaller sensing tubing, making it somewhat more dif-
ficult to achieve the desired consistency in the readings on the
manometer board. If greater care is used in making the tests, com-
parable accuracy should be achieved. It becomes clear from the
figures that velocities below 1 knot cannot be measured accurately
with a manometer board system. It is also clear that there are
little, if any, low Reynolds numbers effects jeopardizing the
measurements at low speeds, particularly on the ½-in. pitot tube.

SHIP AND MODEL DATA

PARTICULARS	MODEL	400-FT SHIP	600-FT SHIP
LENGTH (L_{WL}) FT	20.37	407.4	611.1
LENGTH (L_{BP}) FT	20.00	400.0	600.0
BEAM B FT	2.67	53.40	80.10
DRAFT H FT	1.07	21.40	32.10
DISPLACEMENT TONS	0.950fw	7810sw	26370sw
DESIGN VELOCITY V KNOTS	4.38	19.60	24.0
LCB/L_{WL} AFT OF FP	0.506	0.560	0.560
V/$\sqrt{L_{WL}}$	0.970	0.970	0.970
PROPELLER DIAMETER D FT	0.83	16.60	24.90
ADVANCE COEFFICIENTS J_a	0.922	0.922	0.922

LBP COEFFICIENTS

C_B	0.60
C_P	0.615
C_X	0.977
L_R/L_{WL}	0.50
L/B	7.491
B/H	2.495
$\triangle$ sw/(.01L)^3	122.0
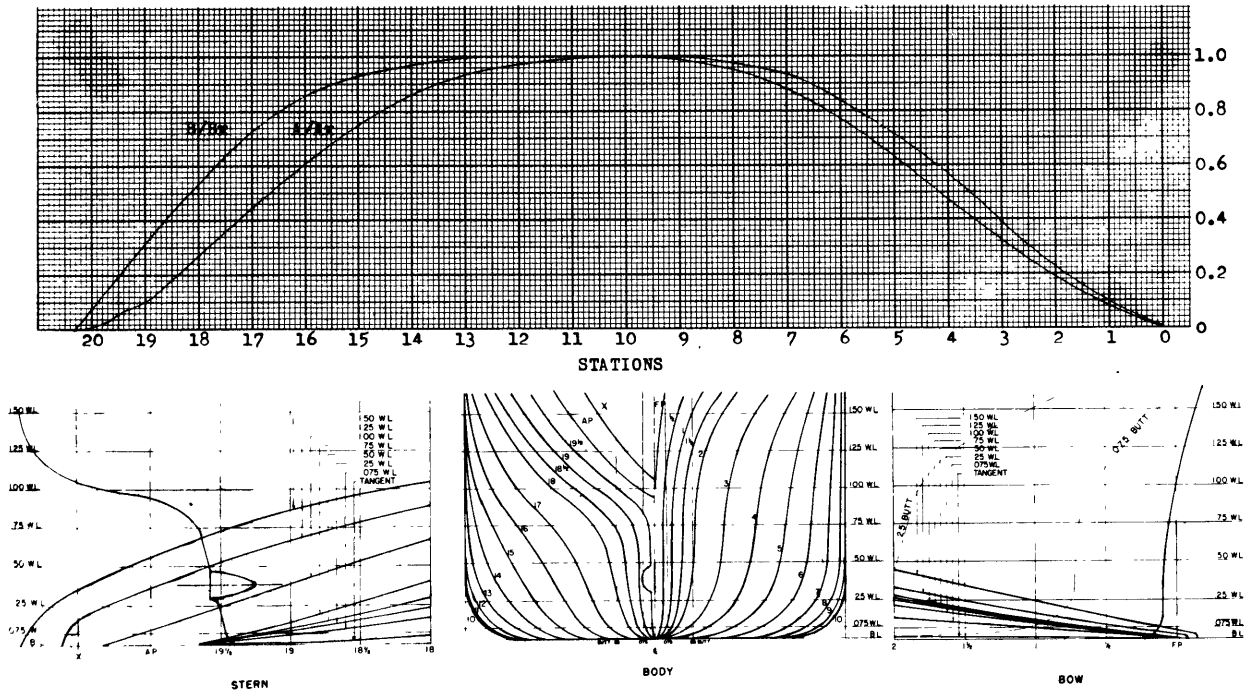
Figure 1 - Ship and Model Data

18

SYSTEM SET FOR RUNNING CONDITION
X = CLAMP

MANIFOLD

MANOMETER BOARD

TANK 1   TANK 2

VACUUM PUMP

MOT   VAC

SOLENOID

STATIONARY GIRDER

TOWING GIRDER

REFERENCE BOTTLE

WATERLINE

PROPELLER SHAFT
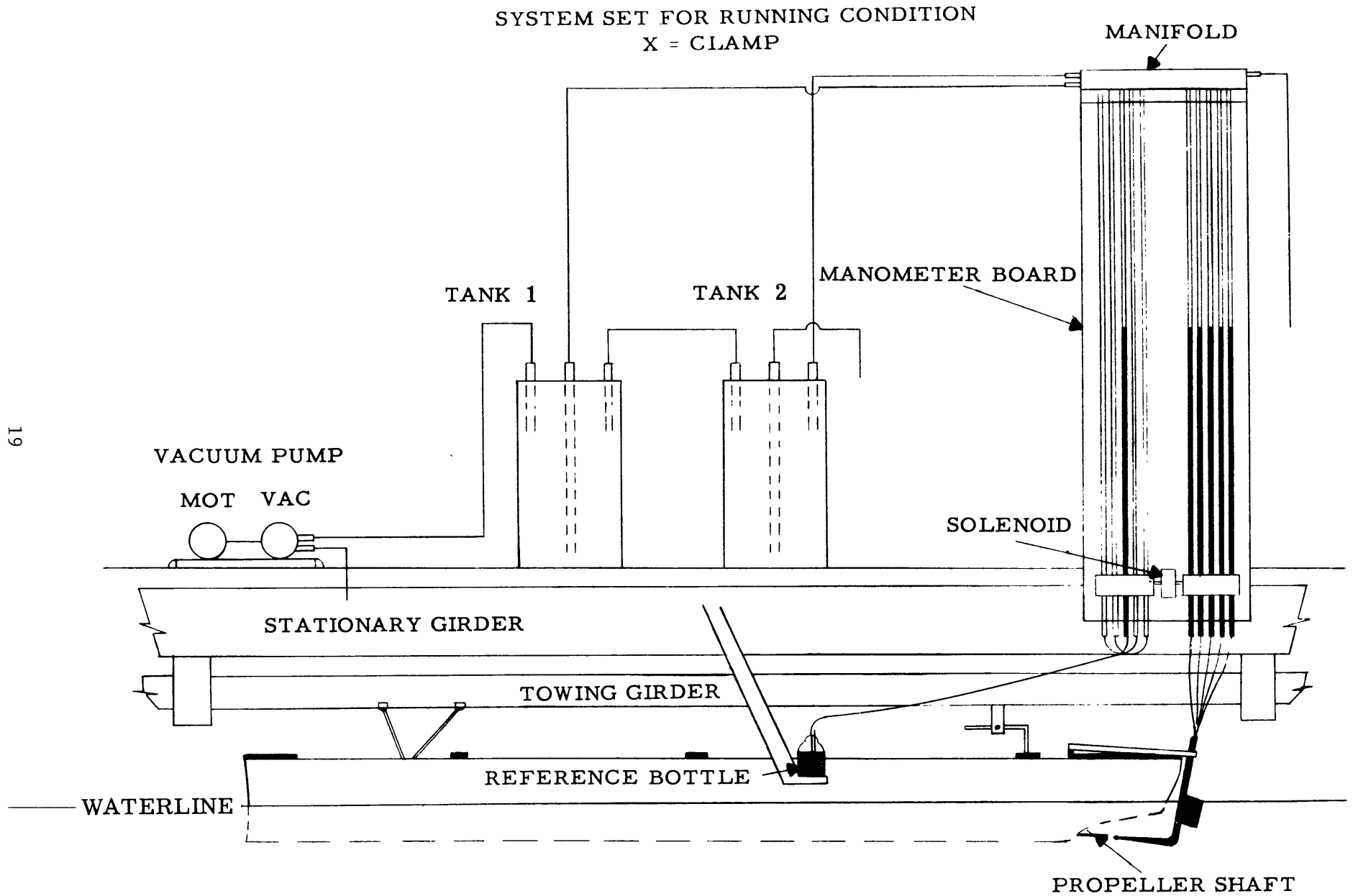
Figure 2   The Pressure System

Propeller 3379 Diameter is 9.954 inches

Propeller Position 1 is 35 percent of propeller diameter
Propeller Position 2 is 15 percent of propeller diameter
Rudder Position A is 71 percent of propeller diameter
Rudder Position B is 50 percent of propeller diameter

Propeller location at Position 1

Propeller location at Position

0.7 propeller radius

1.49"

4.94" 3.48"

7.05"

€ of propellers

€ propeller shaft

Rudder location at Position A

Rudder location at Position B

Figure 3 - Propeller and Rudder Positions

20

SHIP DIMENSIONS	
LENGTH (LWL)	611 1 FT
BEAM	80 0 FT
DRAFT	32 0 FT
TRIM BY STERN	ZERO
DISPLACEMENT	26,350 TONS
PROPELLER DIAMETER	24.89 FT
SPEED	24 0 KT
RUDDER	NONE

TESTS 3P AND 3S
MAY 1964

THE VELOCITY MEASUREMENTS WERE MADE IN A PLANE WHICH IS PERPENDICULAR TO THE CENTERLINE OF THE PROPELLER SHAFT AND INTERSECTS THE SHAFT CENTERLINE 2.4 FT FWD OF THE A.P. (POSITION 1)

r/R — IS THE DISTANCE FROM THE PROPELLER AXIS (r) EXPRESSED AS A RATIO OF THE PROPELLER RADIUS (R).

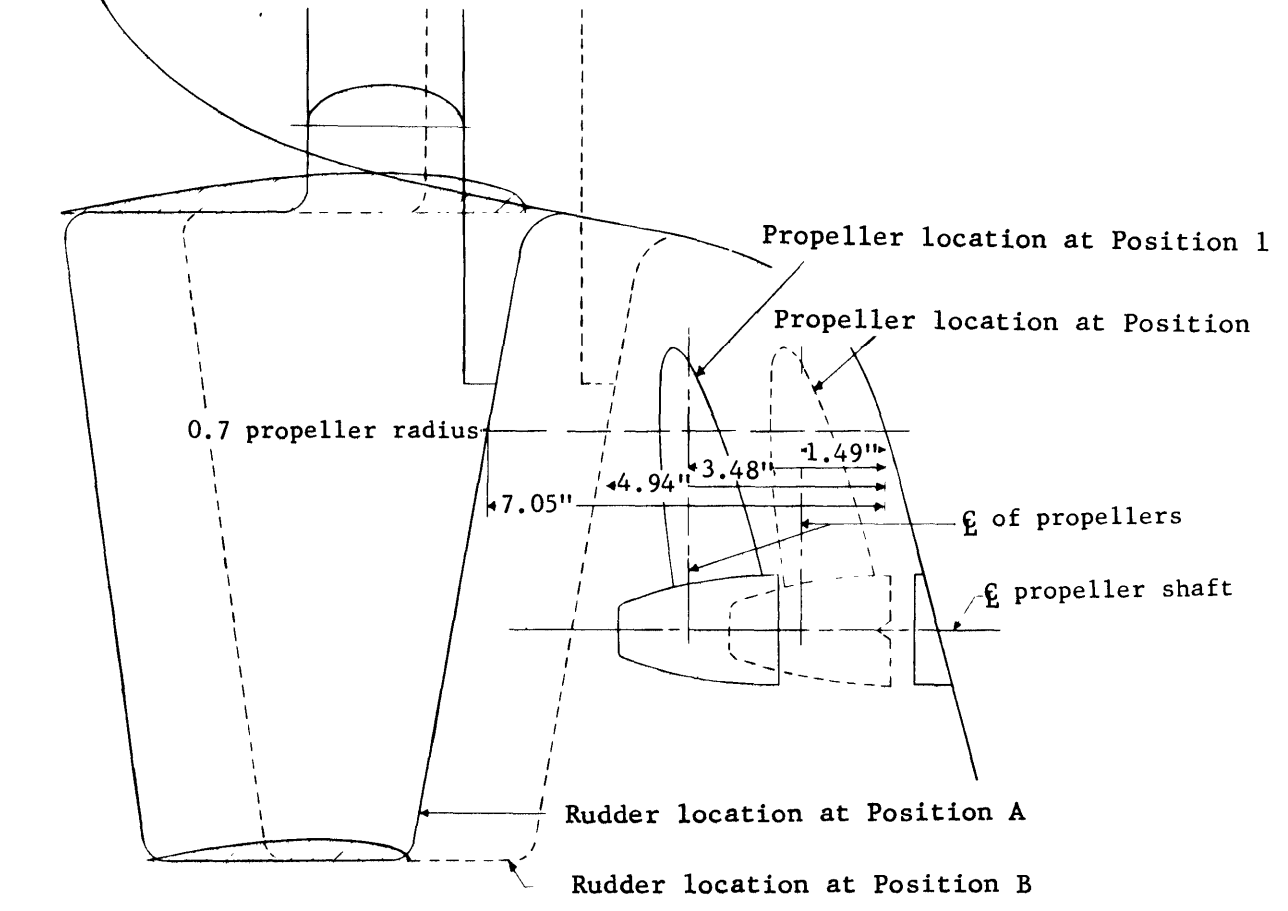θ — IS THE ANGLE MEASURED FROM THE TOP OF THE PROPELLER DISK IN A COUNTERCLOCKWISE DIRECTION

V — IS THE SHIP SPEED.

V_x — IS THE LONGITUDINAL (NORMAL TO THE PLANE OF SURVEY) COMPONENT OF THE WATER VELOCITY AND IS POSITIVE IN THE ASTERN DIRECTION.

V_t — IS THE TANGENTIAL COMPONENT OF THE WATER VELOCITY AND IS POSITIVE IN THE COUNTERCLOCKWISE DIRECTION

V_r — IS THE RADIAL COMPONENT OF THE WATER VELOCITY AND IS POSITIVE TOWARD THE SHAFT CENTERLINE.

V_{tr} — IS THE TRANSVERSE COMPONENT OF THE WATER VELOCITY AND IS THE VECTOR SUM OF V_t AND V_r.

THE VECTOR SHOWN IN THE DIAGRAM IS IN THE DIRECTION OF V_{tr} WITH A MAGNITUDE EQUAL TO V_{tr}/V.

TABLE OF COMPONENT RATIOS

TEST 3P (PORT SIDE) / TEST 3S (STBD SIDE)

POSITION NUMBER	V_x/V	V_T/V	V_R/V	POSITION NUMBER	V_x/V	V_T/V	V_R/V
301	0 384	0	-0 004				
302	0 425	-0.084	-0.017	317	0.486	0.099	-0 121
303	0 465	0.097	-0 010	318	0 545	0 100	-0 019
304	0 517	-0.112	-0.026	319	0 590	0.099	-0 024
305	0.620	-0 121	-0.050	320	0.635	0 114	-0 040
306	0.691	-0 140	-0.054	321	0.738	0 135	-0 060
307	0.747	-0 133	-0 053	322	0 618	0.143	-0.044
308	0 810	-0.128	-0 016	323	0 892	0.149	-0 041
309	0.862	-0.105	0.048	324	0.902	0.121	0 017
310	0 890	-0.063	0 080	325	0 903	0 096	0 044
311	0.890	-0 023	0.088	326	0 907	0.072	0.064
312	0 887	-0.007	0.084	327	0.904	0.063	0.069
313	0.894	-0.004	0 082	328	0 907	0.056	0 068
314	0 887	-0.001	0 079	329	0 904	0 049	0 069
315	0 882	0 010	0 074	330	0.908	0 037	0 071
316	0 889	0	0.075				
201	0 378	0	0.056				
202	0.417	-0 059	0.042	217	0 426	0 072	0 047
203	0.443	-0.076	0 047	218	0.517	0.077	0.026
204	0 519	-0 089	0 032	219	0 537	0 077	0 025
205	0.566	-0 102	0 023	220	0.585	0 092	0 009
206	0.662	-0 126	-0 002	221	0 679	0 116	-0 024
207	0 735	-0.138	-0 022	222	0 723	0 138	-0.025
208	0 841	-0 139	-0.005	223	0.877	0.162	-0 046
209	0.879	-0 116	0 050	224	0.906	0.132	0 009
210	0.905	-0.068	0.086	225	0.898	0 109	0 049
211	0.907	-0 027	0 101	226	0 904	0.087	0 077
212	0.904	-0.011	0.102	227	0 918	0.066	0 098
213	0 906	0.004	0 108	228	0 897	0.013	0.129
214	0 888	0 076	0.140	229	0 732	-0.088	0 106
215	0 694	0.160	0 124	230	0.522	-0 075	0 034
216	0.451	0	0 042				
101	0 391	0	0 092				
102	0 392	-0.025	0 097	117	0.398	0 006	0 100
103	0 393	-0 022	0 097	118	0 409	0.029	0.095
104	0.404	-0 035	0 090	119	0 449	0 031	0 080
105	0.428	-0.046	0 084	120	0.464	0.037	0.071
106	0.510	-0.045	0.058	121	0.487	0.031	0.063
107	0.572	-0.082	0 055	122	0 528	0.042	0 045
108	0.728	-0 128	0.047	123	0 746	0 145	0 011
109	0.822	-0 118	0 090	124	0.807	0.132	0.059
110	0.865	-0 065	0 135	125	0 832	0.101	0.113
111	0 762	0.049	0.158	126	0 668	-0.029	0 116
112	0.634	0 102	0 103	127	0 592	-0.059	0.081
113	0.544	0 102	0.048	128	0 508	-0 066	0 029
114	0.454	0.108	0 012	129	0.449	-0.056	-0 007
115	0 392	0 068	-0.025	130	0 430	-0.026	-0 027
116	0 348	0	-0 047				

(Groups: $r/R = 0.95$, $r/R = 0.70$, $r/R = 0.40$)

VELOCITY SURVEY FOR SERIES 60

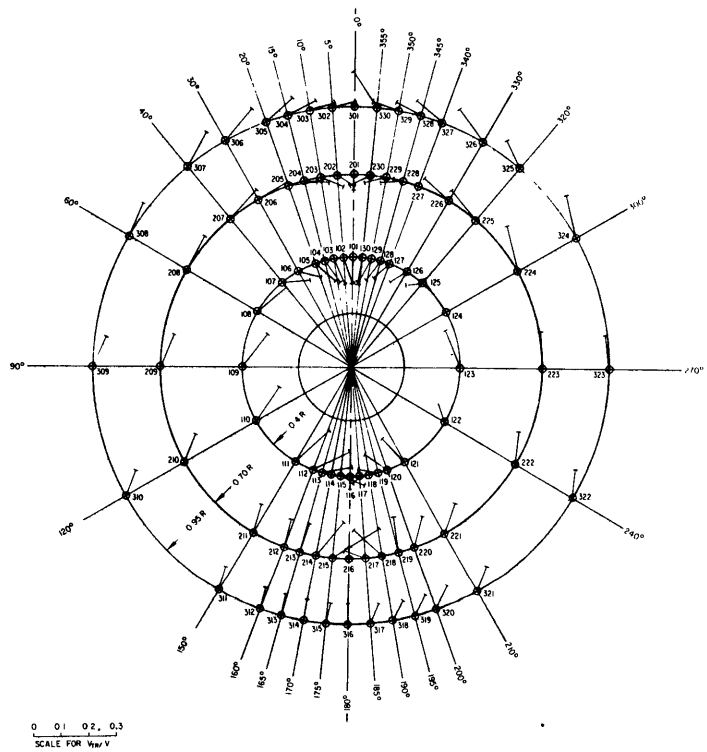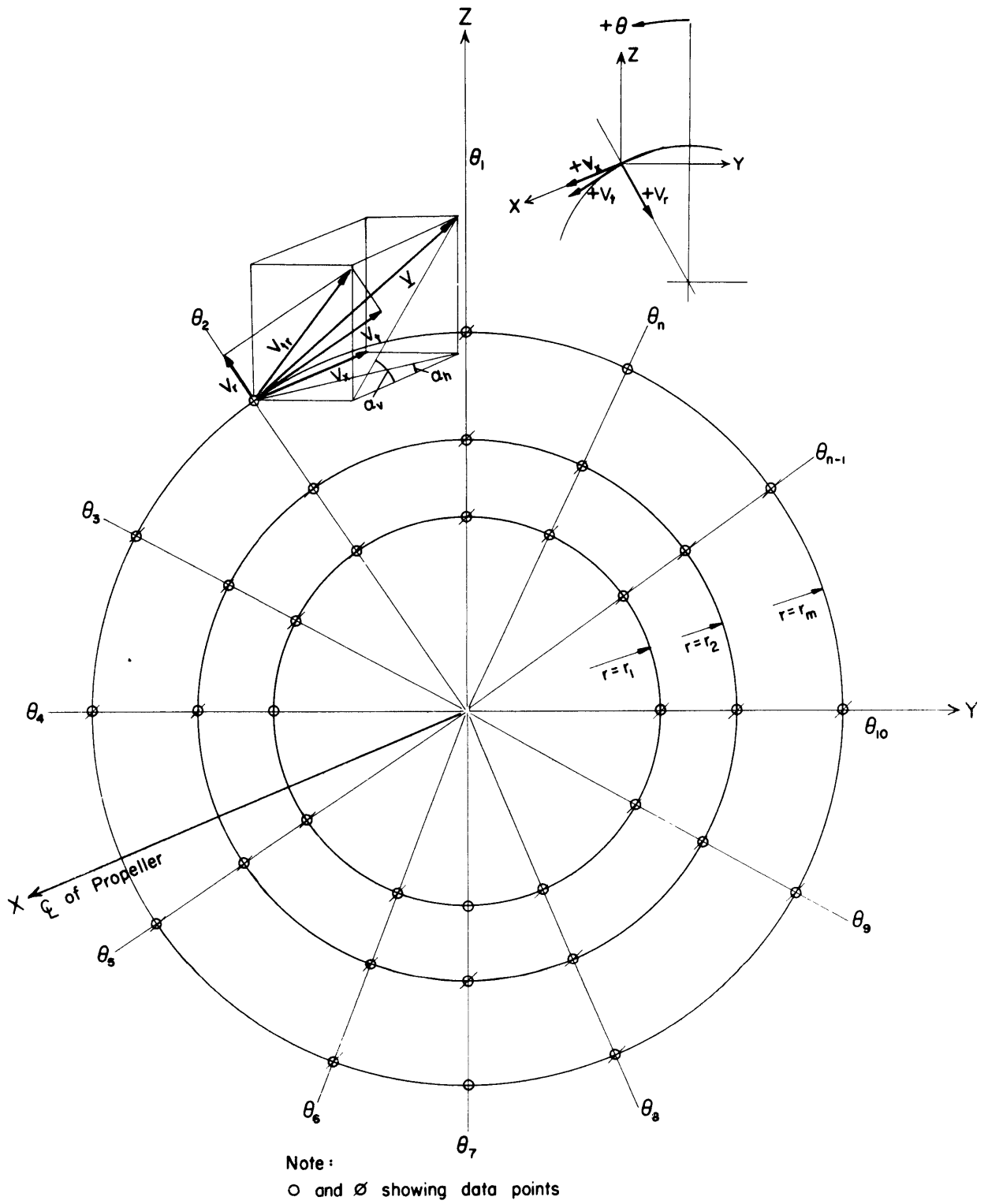
0   0 1   0 2   0.3
SCALE FOR V_{tr}/V

Figure 4 - Velocity Survey in Way of the Propeller for a Hull Design Represented by Model 4210-5

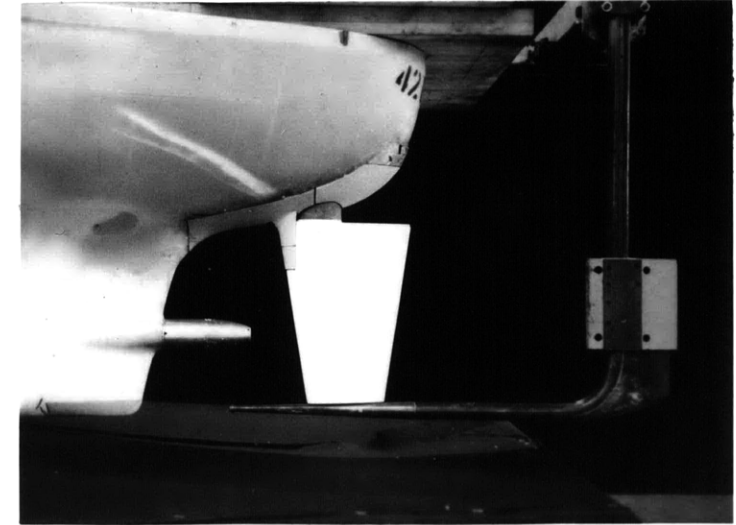Looking Forward

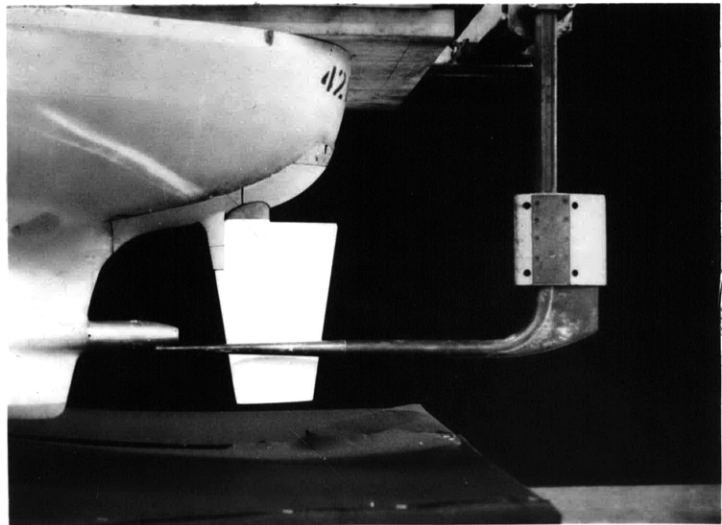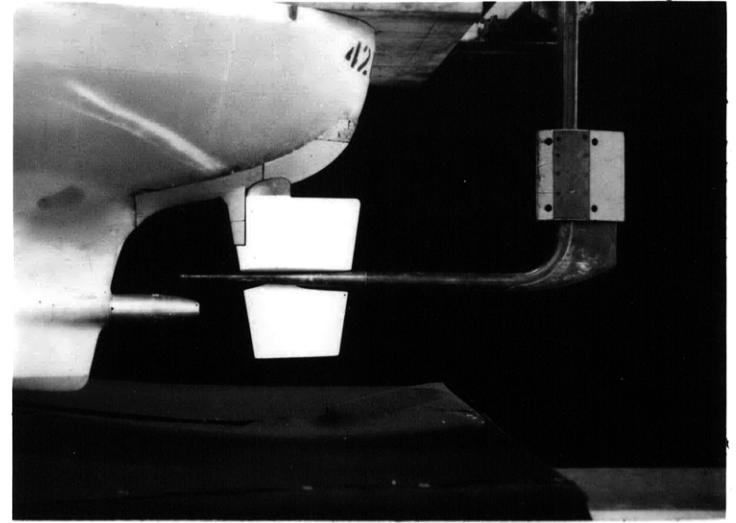Figure 5 - Coordinate System of Velocity Components
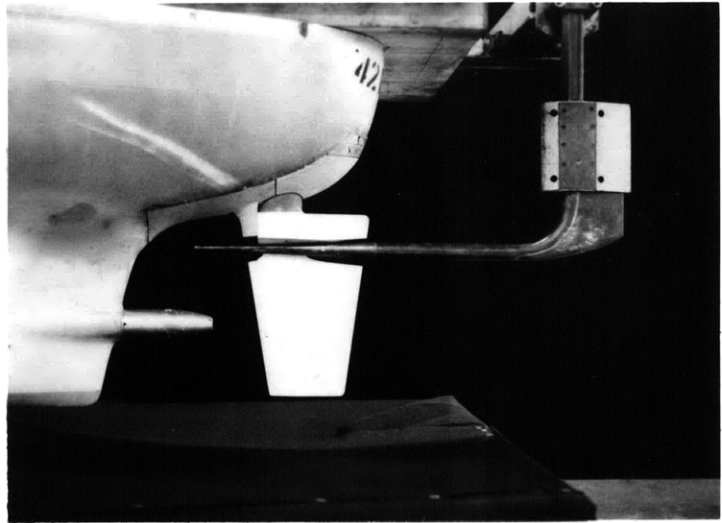
22

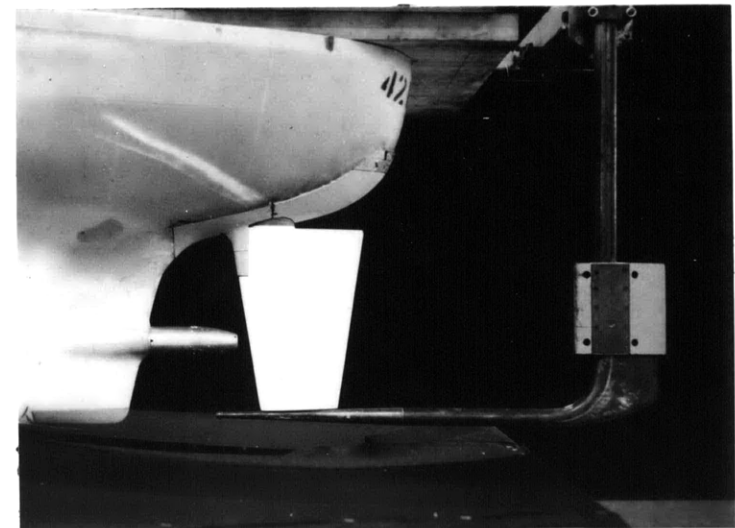Figure 6 - Pitot Tube in Position 1 and Rudder in Position A. Model 4210-5
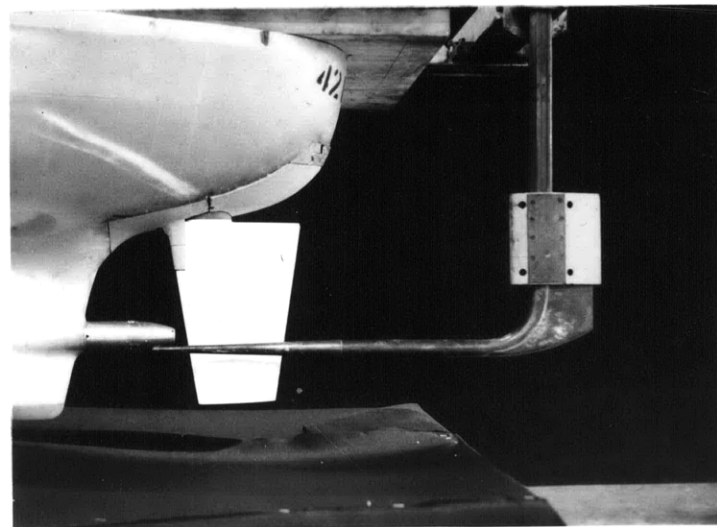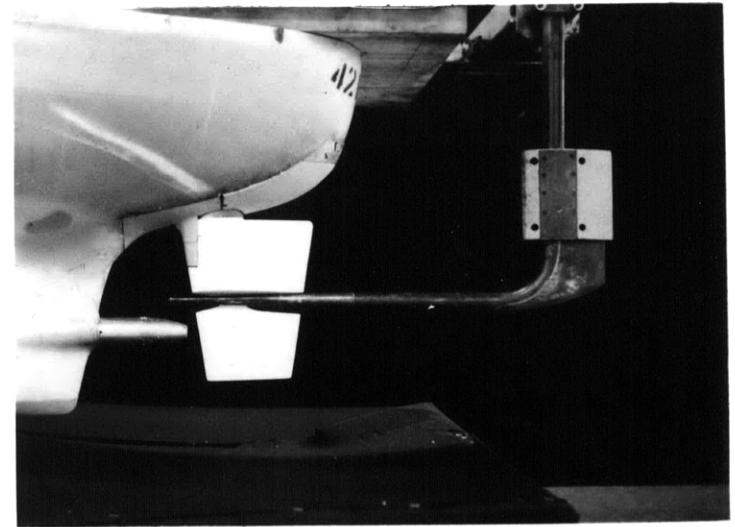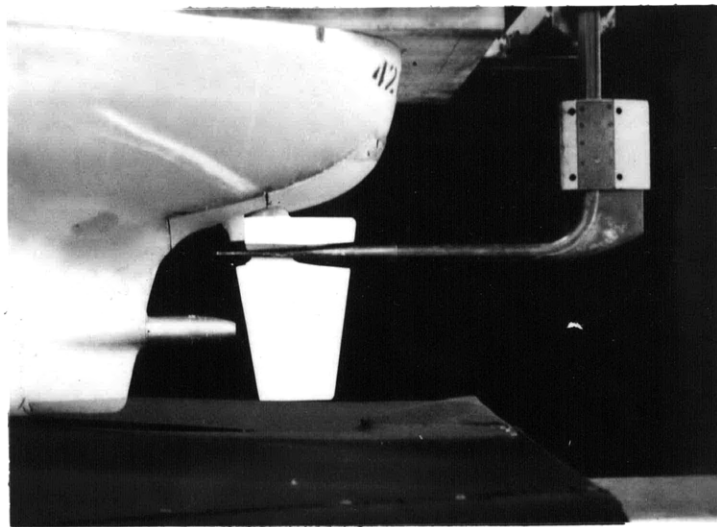
Figure 7 - Pitot Tube in Position 1 and Rudder in Position B, Model 4210-5
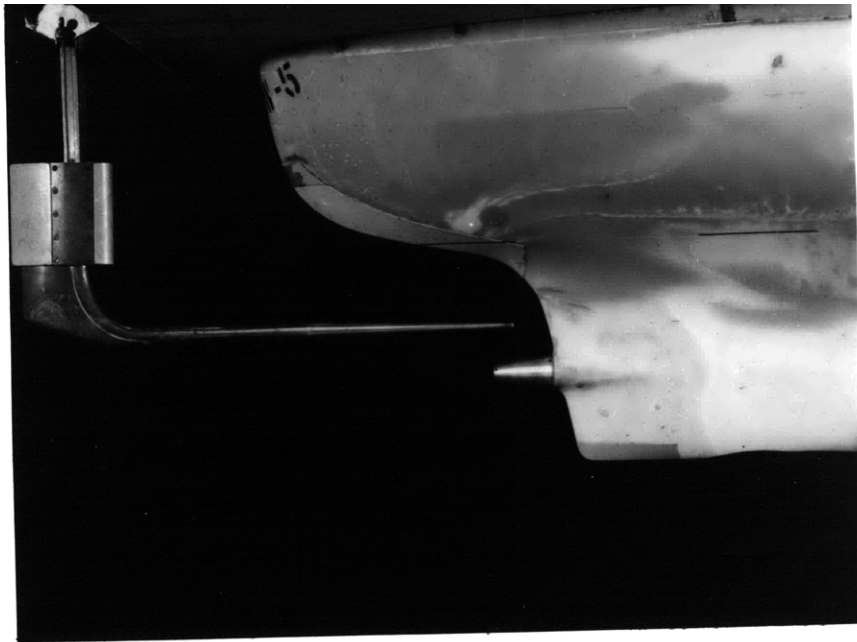
Pitot Tube in Position 2

Rudder Configurations

Figure 8 - Pitot Tube and Some of the Rudder Configurations Used
for Wake Survey with Model 4210-5

SYMBOL	TEST NUMBER	TUBE POSITION	RUDDER POSITION	SPEED (KNOTS)	DISPLACEMENT (POUNDS)	TRIM (FEET)
——○——	3P	1	none	4.38	2127	zero
——△——	1	2	none	4.38	1489	0.48 x stern

Figure 9 - Circumferential Longitudinal (V_x/V) and Tangential (V_t/V) Velocity Distribution at Test Radii Due to Variations in Longitudinal Position of Plane of Survey, Displacement, and Trim, Model 4210-5

SYMBOL	TEST NUMBER	TUBE POSITION	RUDDER POSITION	SPEED (KNOTS)	DISPLACEMENT (POUNDS)	TRIM
─○─	3P	I	none	4.38	2127	zero
─ ─△─ ─	2	I	none	3.90	2127	zero
─··─☐─··─	4	I	none	5.10	2127	zero

Figure 10 - Circumferential Longitudinal (V_x/V) and Tangential (V_t/V) Velocity Distribution at Test Radii Due to Variations in Model Speed, Model 4210-5

SYMBOL	TEST NUMBER	TUBE POSITION	RUDDER POSITION	SPEED (KNOTS)	DISPLACEMENT (POUNDS)	TRIM
⊖	3P	I	none	4.38	2127	zero
⊟	3PR	I	none	4.38	2127	zero
△	3S	I	none	4.38	2127	zero

Figure 11 - Circumferential Longitudinal (V_x/V) and Tangential (V_t/V) Velocity Distribution at Test Radii Due to Asymmetries and Repeatability, Model 4210-5

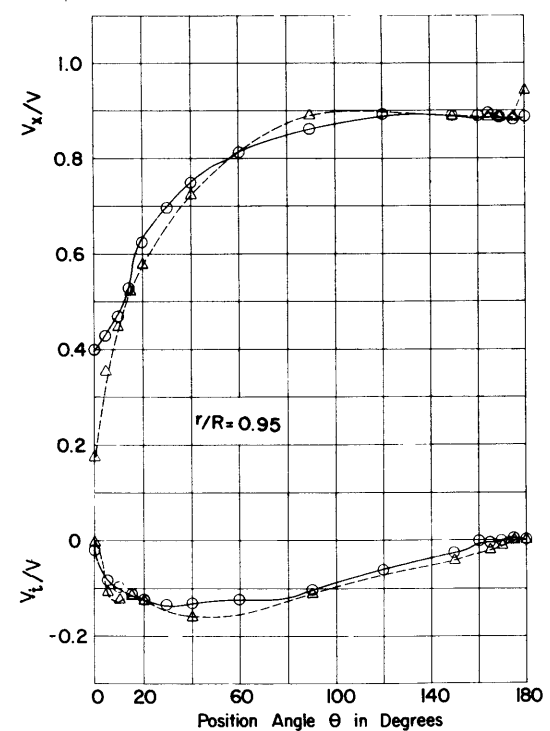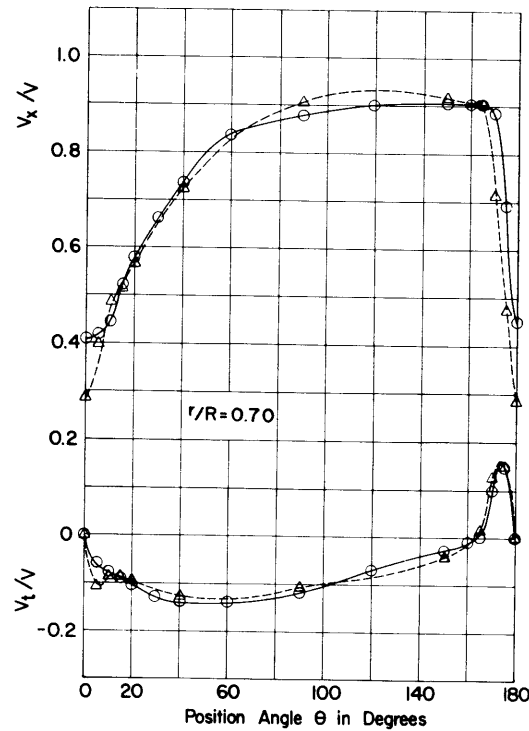| SYMBOL	TEST NUMBER	TUBE POSITION	RUDDER POSITION	SPEED (KNOTS)	DISPLACEMENT (POUNDS)	TRIM
—⊖—	3P	I	none	4.38	2127	zero
—△——	5	I	B	4.38	2127	zero
—⊟——	6	I	A	4.38	2127	zero

r/R=0.40

r/R=0.70

r/R=0.95
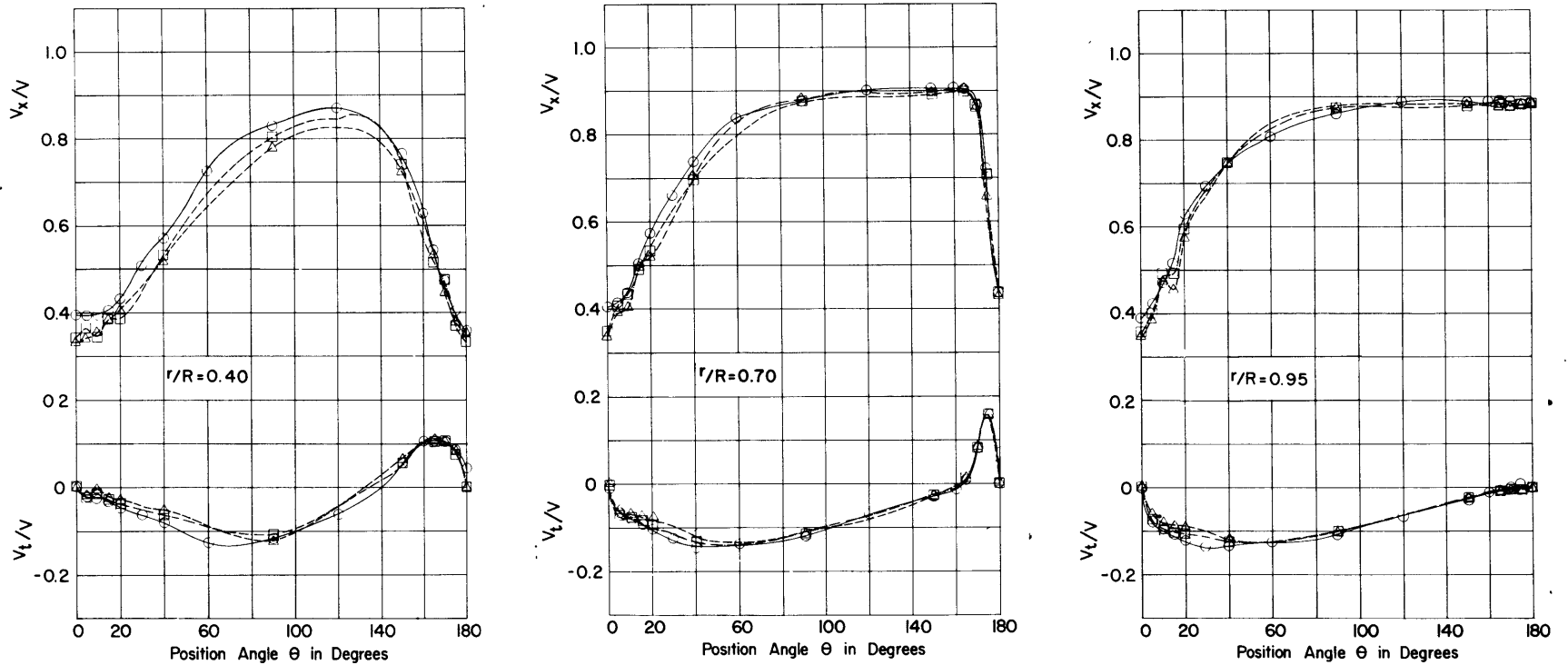
Figure 12 - Circumferential Longitudinal (V_x/V) and Tangential (V_t/V) Velocity

Distribution at Test Radii Due to Variations in Longitudinal

Position of Rudder, Model 4210-5

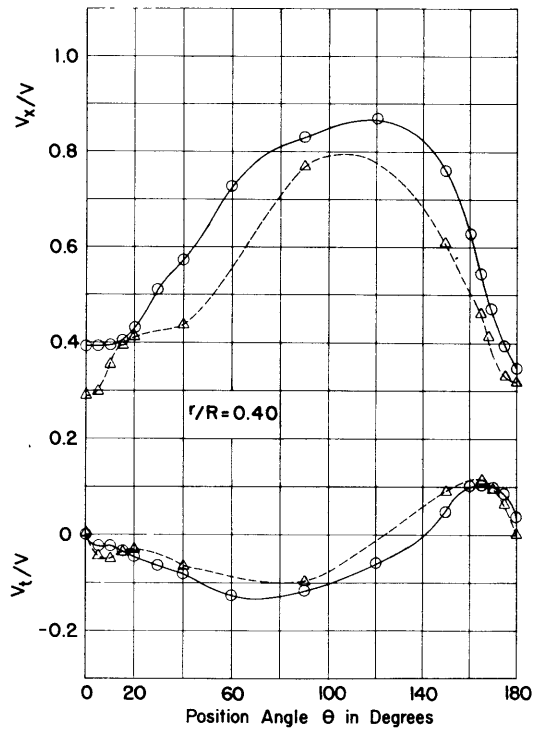| SYMBOL	TEST NUMBER	TUBE POSITION	RUDDER POSITION	SPEED (KNOTS)	DISPLACEMENT (POUNDS)	TRIM
—⊖—	3P	1	none	4.38	2127	zero
--△--	7	2	none	4.38	2127	zero
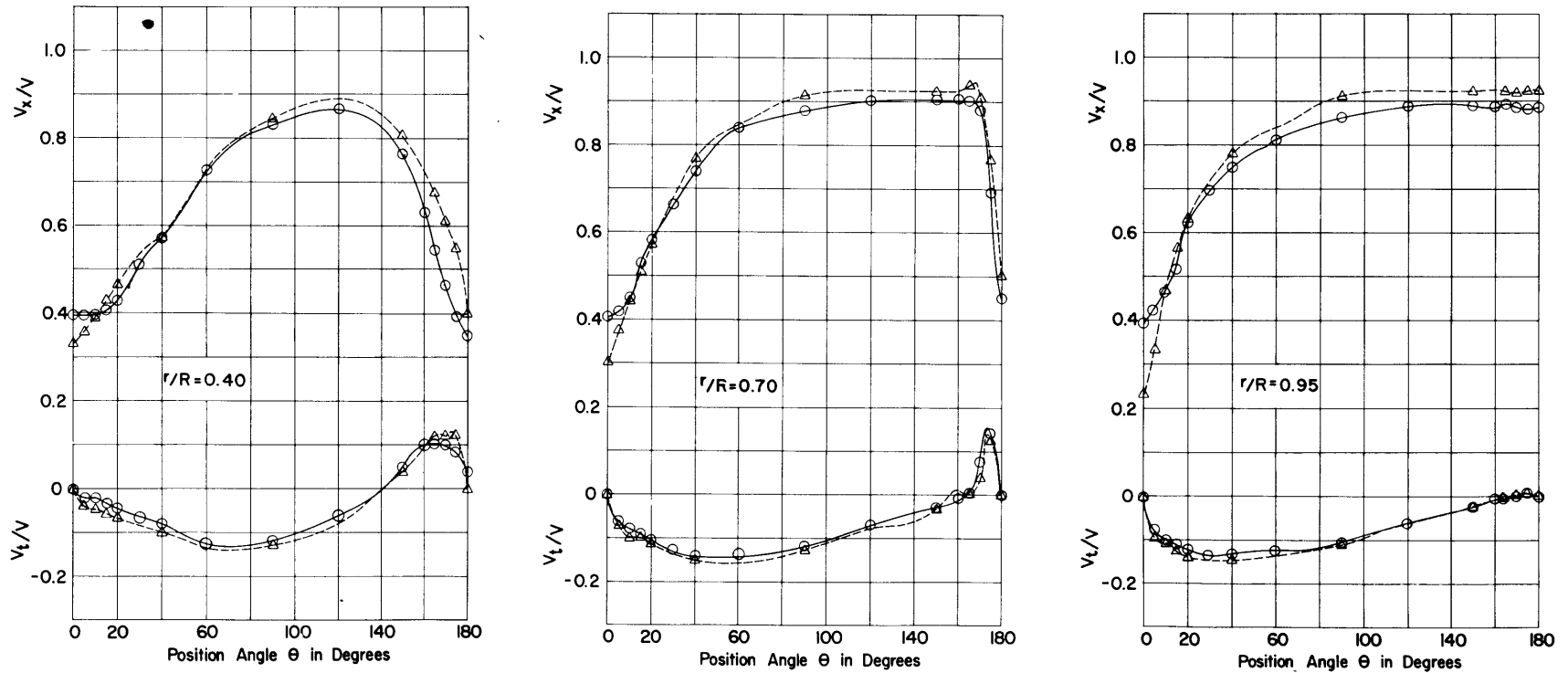
Figure 13 - Circumferential Longitudinal (V_x/V) and Tangential (V_t/V) Velocity
Distribution at Test Radii Due to Variations in Longitudinal
Position of Plane of Survey, Model 4210-5

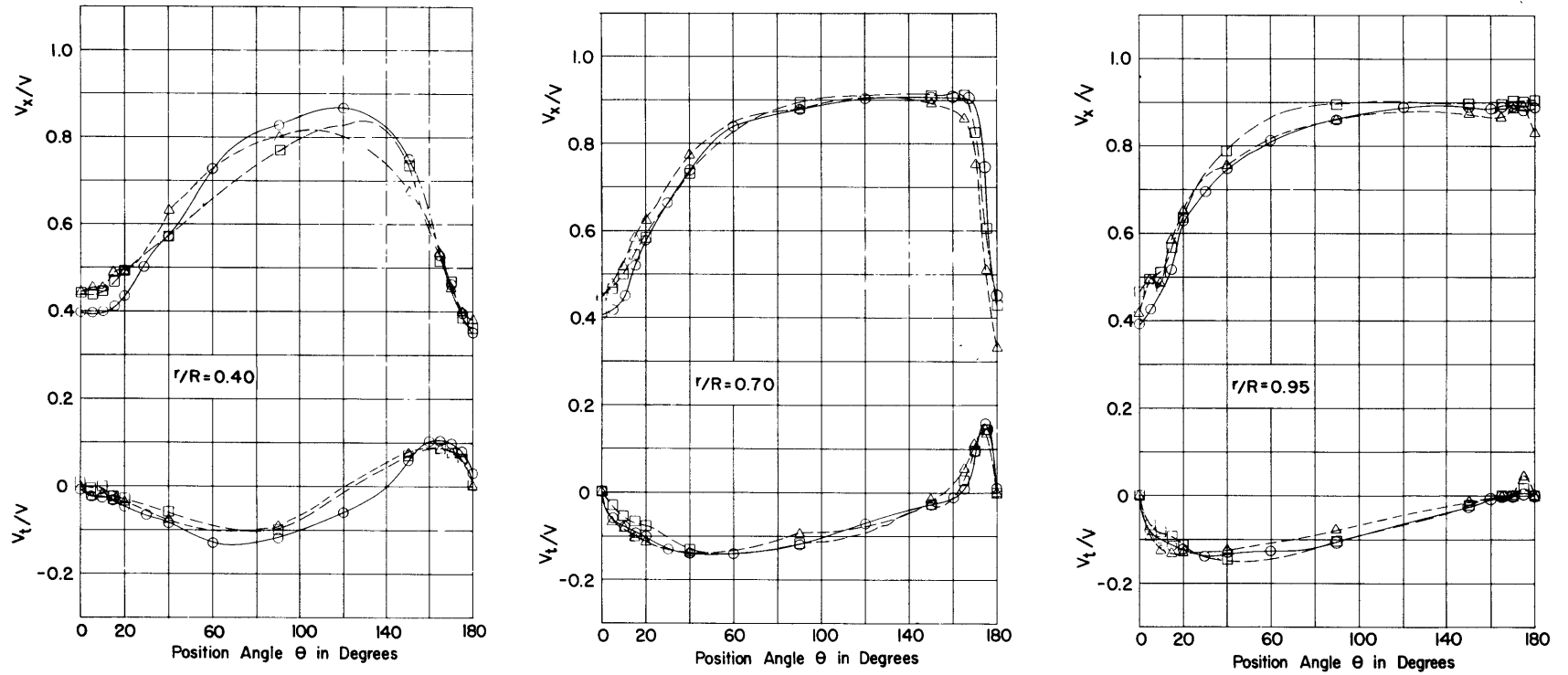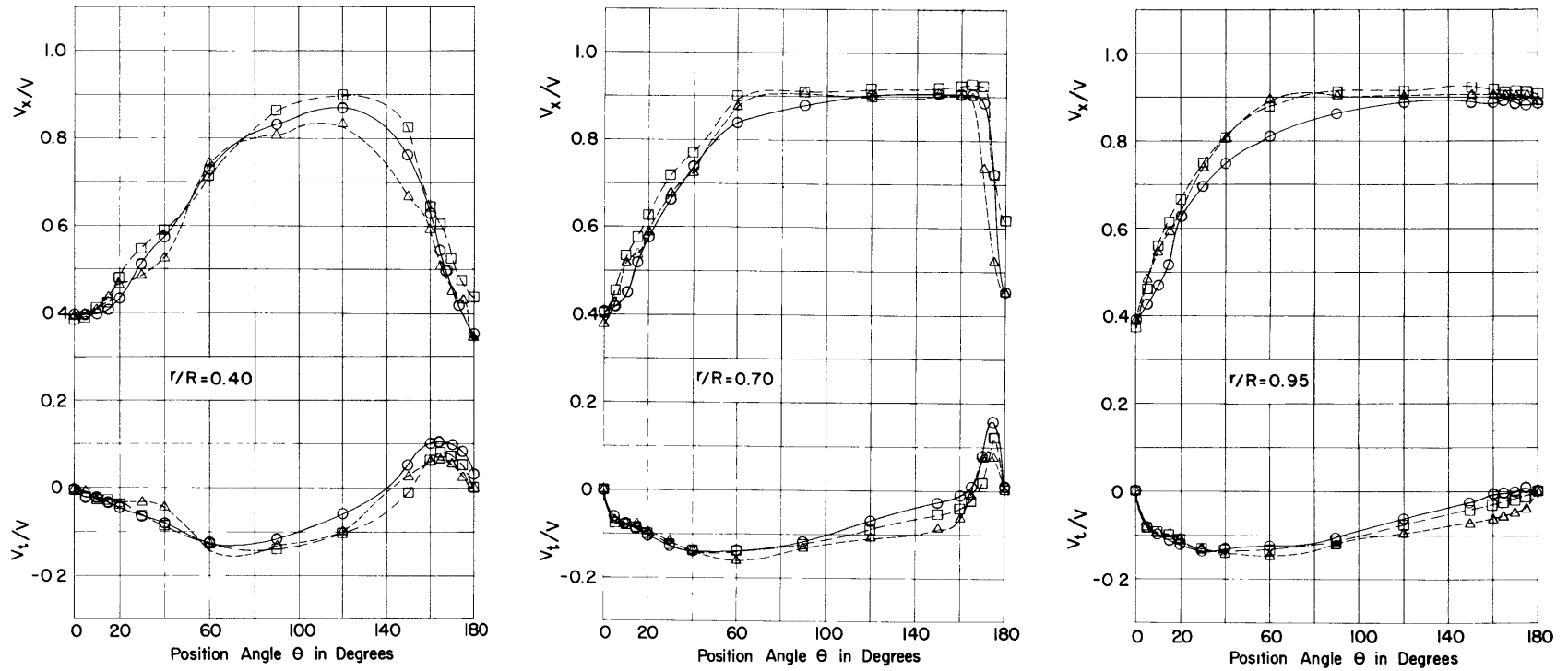| SYMBOL	TEST NUMBER	TUBE POSITION	RUDDER POSITION	SPEED (KNOTS)	DISPLACEMENT (POUNDS)	TRIM (FEET)
───⊖───	3P	I	none	4.38	2127	zero
──△──	8	I	none	4.38	1276	0.48 x stern
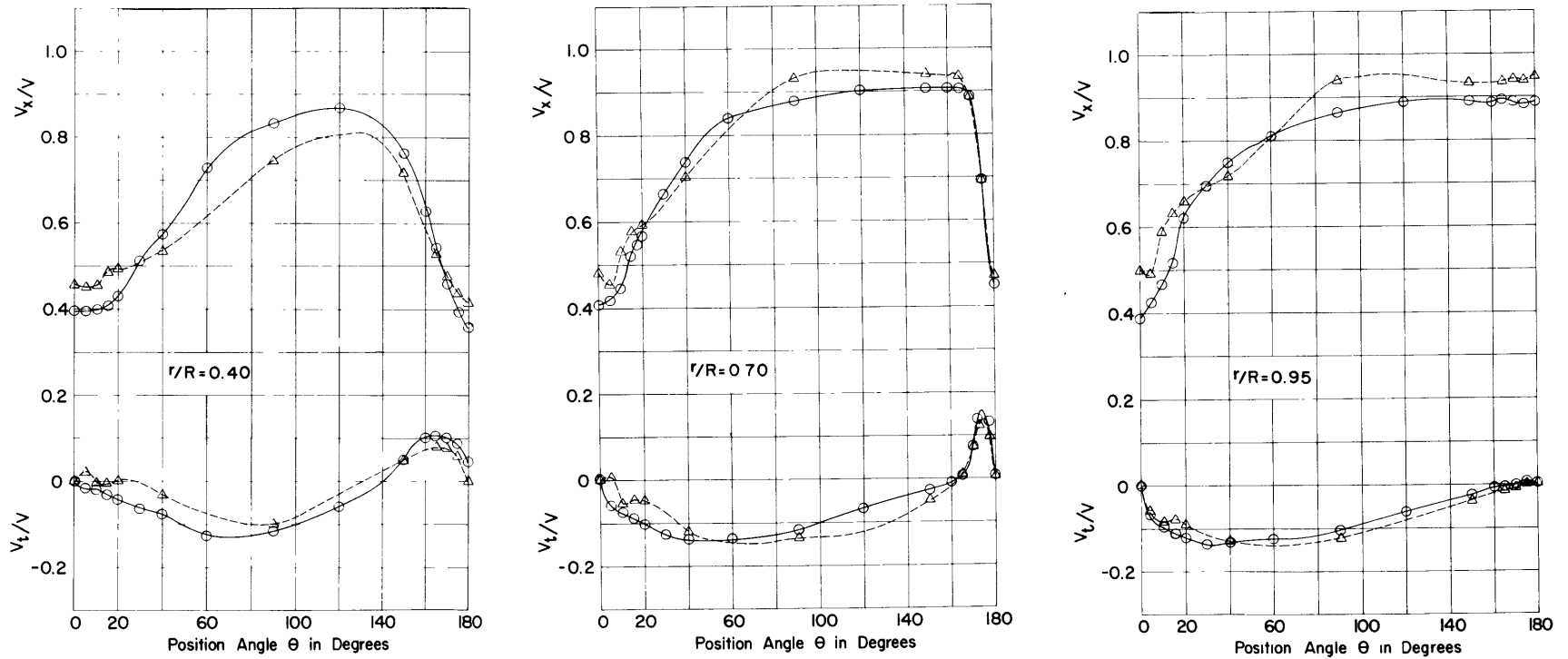
Figure 14 - Circumferential Longitudinal (V_x/V) and Tangential (V_t/V) Velocity
Distribution at Test Radii Due to Variations in Displacement
and Trim, Model 4210-5

Figure 15 - Calculated Volumetric Velocity ($\overline{V}_V/V$), Volumetric Mean Wake Velocity (1-W_x), and Mean Longitudinal Velocity ($\overline{V}_x/V$) Showing Differences Due to Variations in Longitudinal Position of Plane of Survey, Displacement, and Trim, Model 4210-5

Figure 16 - Calculated Volumetric Velocity ($\overline{V}_V/V$), Volumetric Mean Wake Velocity ($1-W_x$), and Mean Longitudinal Velocity ($\overline{V}_x/V$) Showing Differences Due to Variations in Model Speed, Model 4210-5

Figure 17 - Calculated Volumetric Velocity ($\overline{V}_V/V$), Volumetric Mean Wake Velocity ($1-W_x$), and Mean Longitudinal Velocity ($\overline{V}_x/V$) Showing Differences Due to Asymmetries and Repeatability, Model 4210-5

34

Figure 18 - Calculated Volumetric Velocity $(\overline{V}_V/V)$, Volumetric Mean Wake Velocity $(1-W_x)$, and Mean Longitudinal Velocity $(\overline{V}_x/V)$ Showing Differences Due to Variations in Longitudinal Position of Rudder, Model 4210-5

35

SYMBOL	TEST NUMBER	TUBE POSITION	RUDDER POSITION	SPEED (KNOTS)	DISPLACEMENT (POUNDS)	TRIM
—○—	3P	I	none	4.38	2127	zero
—△—	7	2	none	4.38	2127	zero

Figure 19 - Calculated Volumetric Velocity ($\overline{V}_v/V$), Volumetric Mean Wake
Velocity ($1-W_x$), and Mean Longitudinal Velocity ($\overline{V}_x/V$) Showing
Differences Due to Variations in Longitudinal Position
of Plane of Survey, Model 4210-5

36

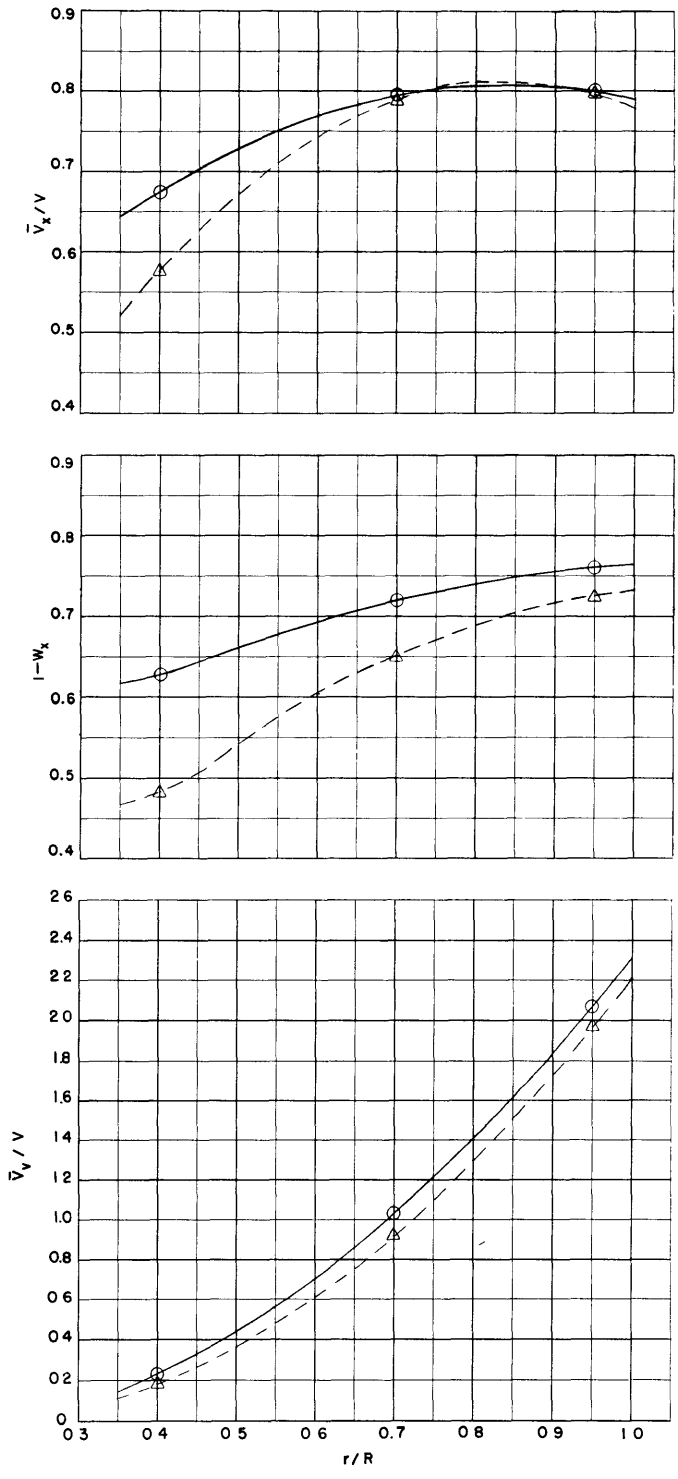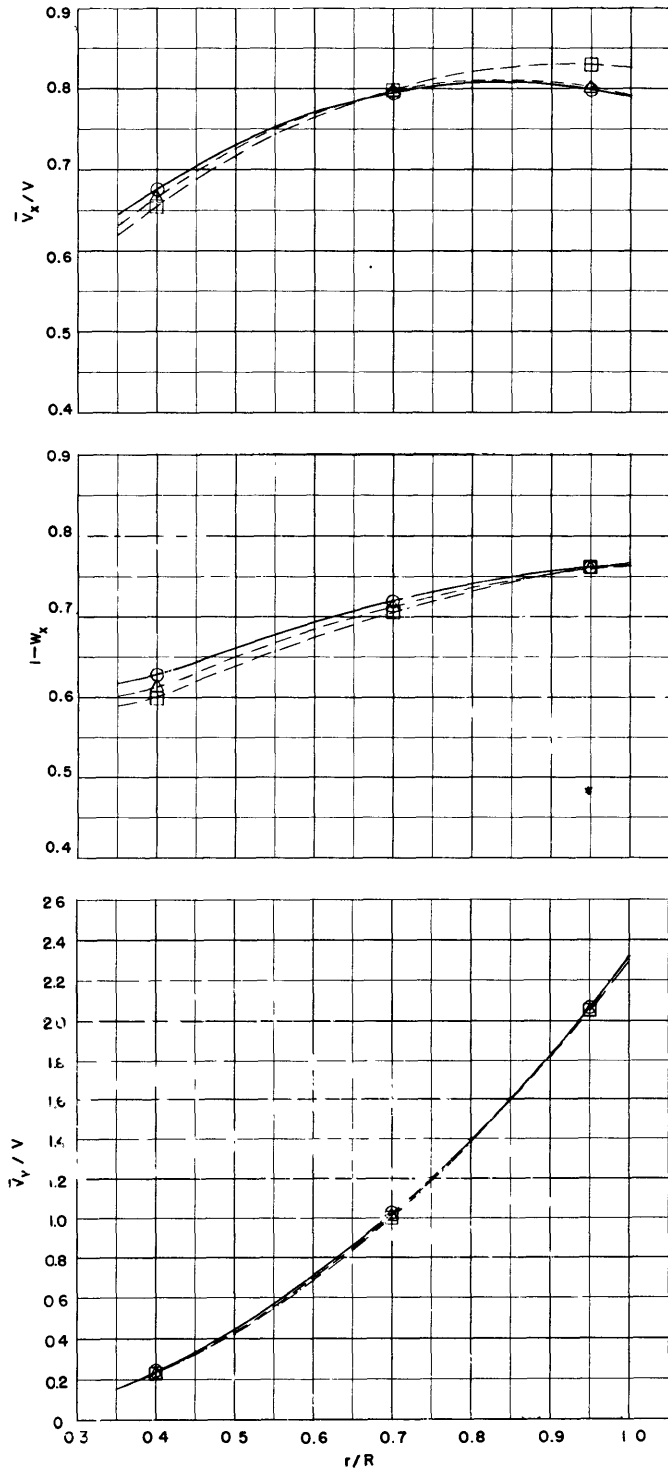| SYMBOL	TEST NUMBER	TUBE POSITION	RUDDER POSITION	SPEED (KNOTS)	DISPLACEMENT (POUNDS)	TRIM (FEET)
—○—	3P	I	none	4.38	2127	zero
—△—	8	I	none	438	1276	0 48 x stern

Figure 20 - Calculated Volumetric Velocity ($\overline{V}_V/V$), Volumetric Mean Wake Velocity ($1-W_x$), and Mean Longitudinal Velocity ($\overline{V}_x/V$) Showing Differences Due to Variations in Displacement and Trim, Model 4210-5

37

HARMONIC AMPLITUDES
DERIVED FROM ANALYSIS OF THE
LONGITUDINAL COMPONENT OF VELOCITY RATIOS
FOR A HULL DESIGN REPRESENTED BY
MODEL 4210-5

SHIP DIMENSIONS

LENGTH (LWL)	611.1	FT
BEAM	80.0	FT
DRAFT	32.0	FT, E.K.
DISPLACEMENT	26,350	TONS
PROPELLER DIAMETER	24.89	FT
SPEED	24.0	KNOTS

TEST 3P
MAY 1964

r/R	SYMBOL
0.3	O
0.5	□
0.7	△
0.9	◇
1.0	+

SINGLE AMPLITUDE (C_n)

HARMONIC OF SHAFT FREQUENCY (n)
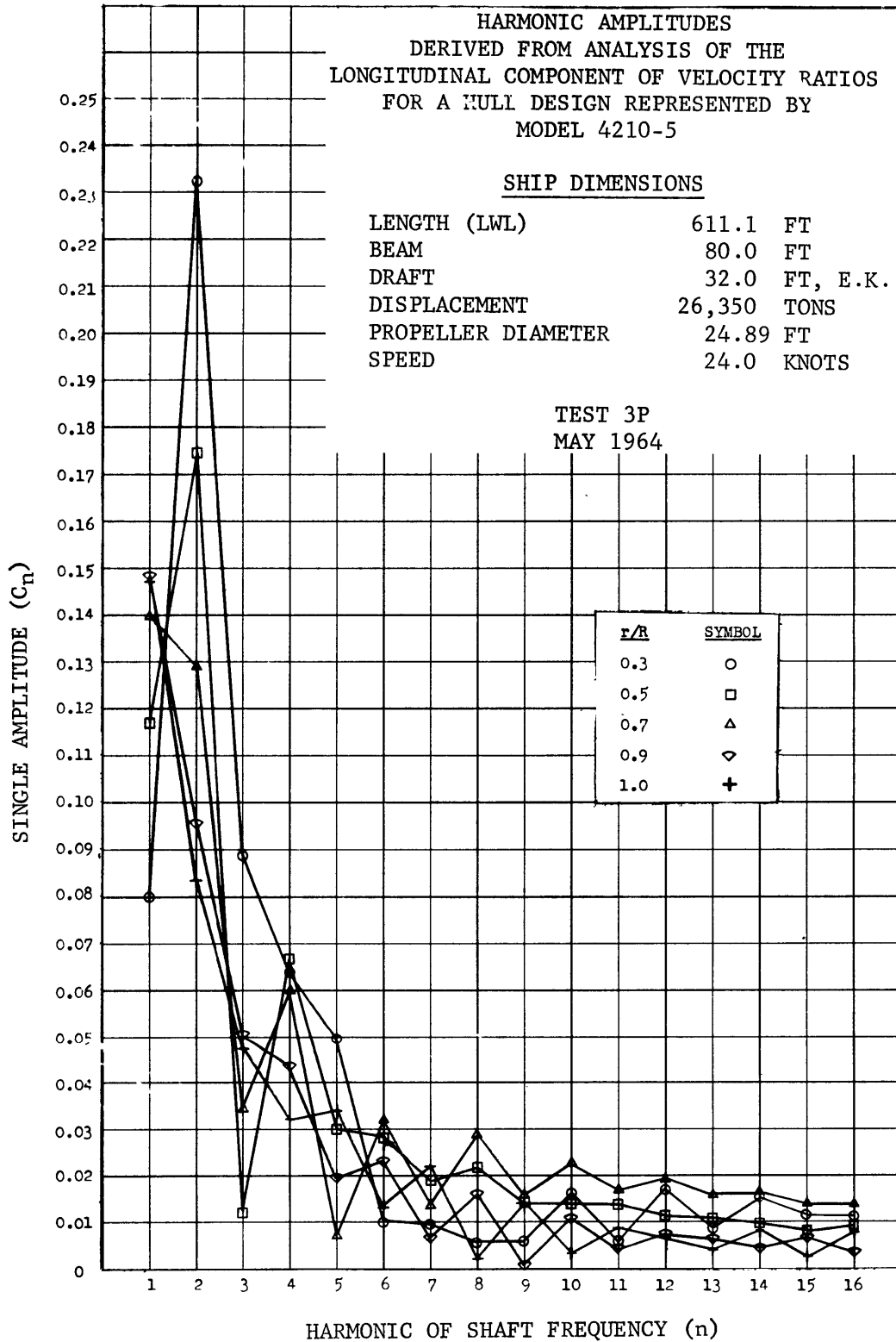
Figure 21 - Harmonic of Shaft Frequency (n)

38

AMPLITUDE OF nth HARMONICS

$\left(\dfrac{\tilde{V}_x}{V}\right)_{5th}$ $n=5$

SYMBOL	TEST NUMBER	TUBE POSITION	RUDDER POSITION	SPEED (KNOTS)	DISPLACEMENT (POUNDS)	TRIM (FEET)
——	3P	1	none	4.38	2127	zero
– – –	1	2	none	4.38	1489	0.48 x stern

AMPLITUDE OF nth HARMONICS

$\left(\dfrac{\tilde{V}_x}{V}\right)_{1st}$ $n=1$

$\left(\dfrac{\tilde{V}_x}{V}\right)_{6th}$ $n=6$

$\left(\dfrac{\tilde{V}_x}{V}\right)_{3rd}$ $n=3$

$\left(\dfrac{\tilde{V}_x}{V}\right)_{7th}$ $n=7$

$\left(\dfrac{\tilde{V}_x}{V}\right)_{4th}$ $n=4$

$\left(\dfrac{\tilde{V}_x}{V}\right)_{8th}$ $n=8$

r/R

Figure 22 - Amplitudes of Harmonics of Longitudinal Velocity Components $(\tilde{V}_x/V)$ Showing Differences Due to Variations in Longitudinal Position of Plane of Survey, Displacement, and Trim, Model 4210-5

39

AMPLITUDE OF nth HARMONICS

SYMBOL	TEST NUMBER	TUBE POSITION	RUDDER POSITION	SPEED (KNOTS)	DISPLACEMENT (POUNDS)	TRIM
——	3P	I	none	4.38	2127	zero
— — —	2	I	none	3.90	2127	zero
—·—	4	I	none	5.10	2127	zero

$\left(\frac{\tilde{V}_x}{V}\right)_{5th}$ n=5

$\left(\frac{\tilde{V}_x}{V}\right)_{6th}$ n=6

$\left(\frac{\tilde{V}_x}{V}\right)_{7th}$ n=7

$\left(\frac{\tilde{V}_x}{V}\right)_{8th}$ n=8

AMPLITUDE OF nth HARMONICS

$\left(\frac{\tilde{V}_x}{V}\right)_{1st}$ n=1

$\left(\frac{\tilde{V}_x}{V}\right)_{3rd}$ n=3

$\left(\frac{\tilde{V}_x}{V}\right)_{4th}$ n=4

r/R

Figure 23 - Amplitudes of Harmonics of Longitudinal Velocity Components $(\tilde{V}_x/V)$ Showing Differences Due to Variations in Model Speed, Model 4210-5

40

$\left(\dfrac{\tilde{V}_x}{V}\right)5^{th}$ n = 5

SYMBOL	TEST NUMBER	TUBE POSITION	RUDDER POSITION	SPEED (KNOTS)	DISPLACEMENT (POUNDS)	TRIM
——	3P	I	none	4.38	2127	zero
—·—	3PR	I	none	4.38	2127	zero
———	3S	I	none	4.38	2127	zero

AMPLITUDE OF nth HARMONICS

$\left(\dfrac{\tilde{V}_x}{V}\right)1^{st}$ n = 1

$\left(\dfrac{\tilde{V}_x}{V}\right)6^{th}$ n = 6

$\left(\dfrac{\tilde{V}_x}{V}\right)3^{rd}$ n = 3

$\left(\dfrac{\tilde{V}_x}{V}\right)7^{th}$ n = 7

$\left(\dfrac{\tilde{V}_x}{V}\right)4^{th}$ n = 4

$\left(\dfrac{\tilde{V}_x}{V}\right)8^{th}$ n = 8

r/R

Figure 24 - Amplitudes of Harmonics of Longitudinal Velocity Components $(\tilde{V}_x/V)$ Showing Differences Due to Asymmetries and Repeatability, Model 4210-5

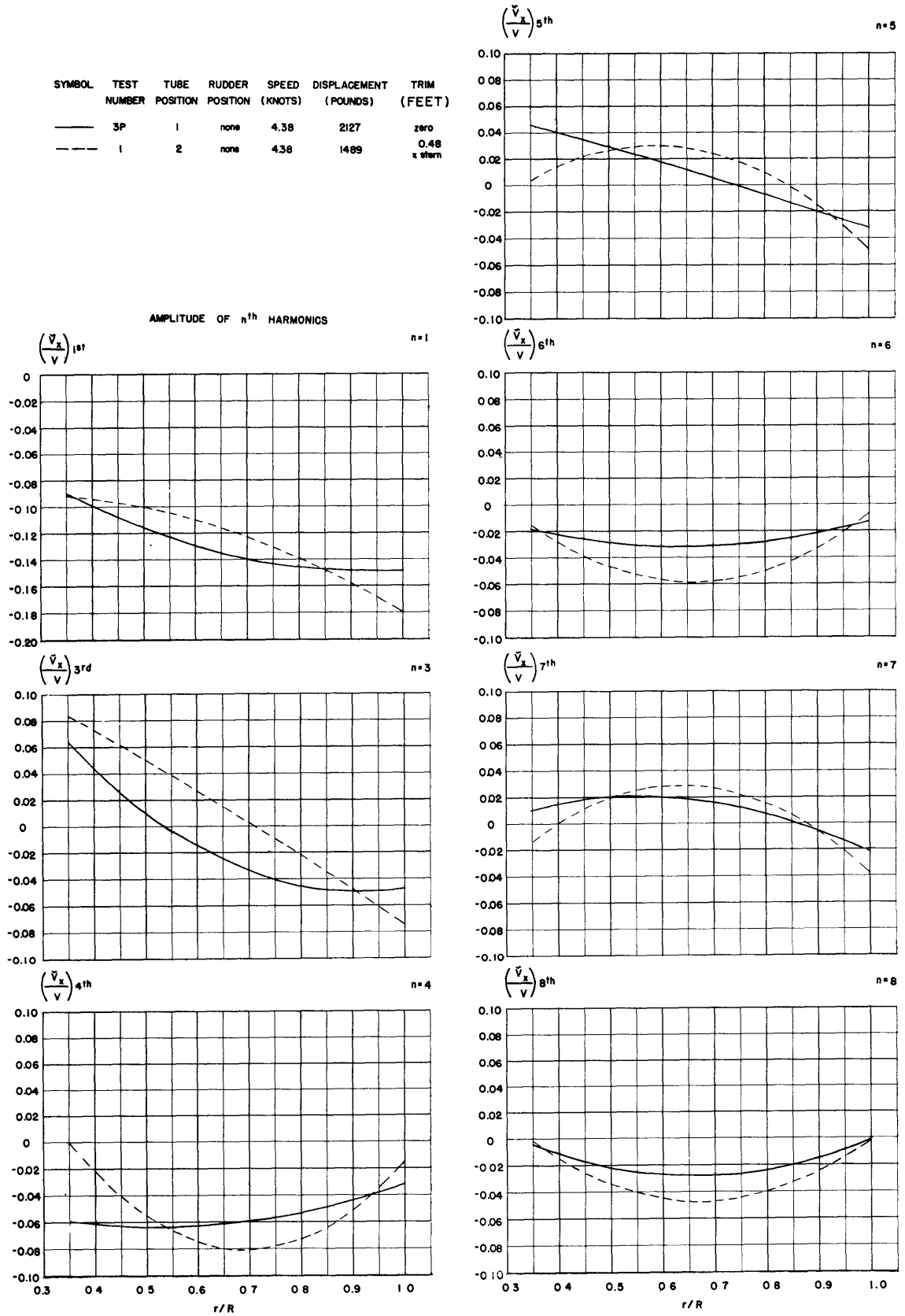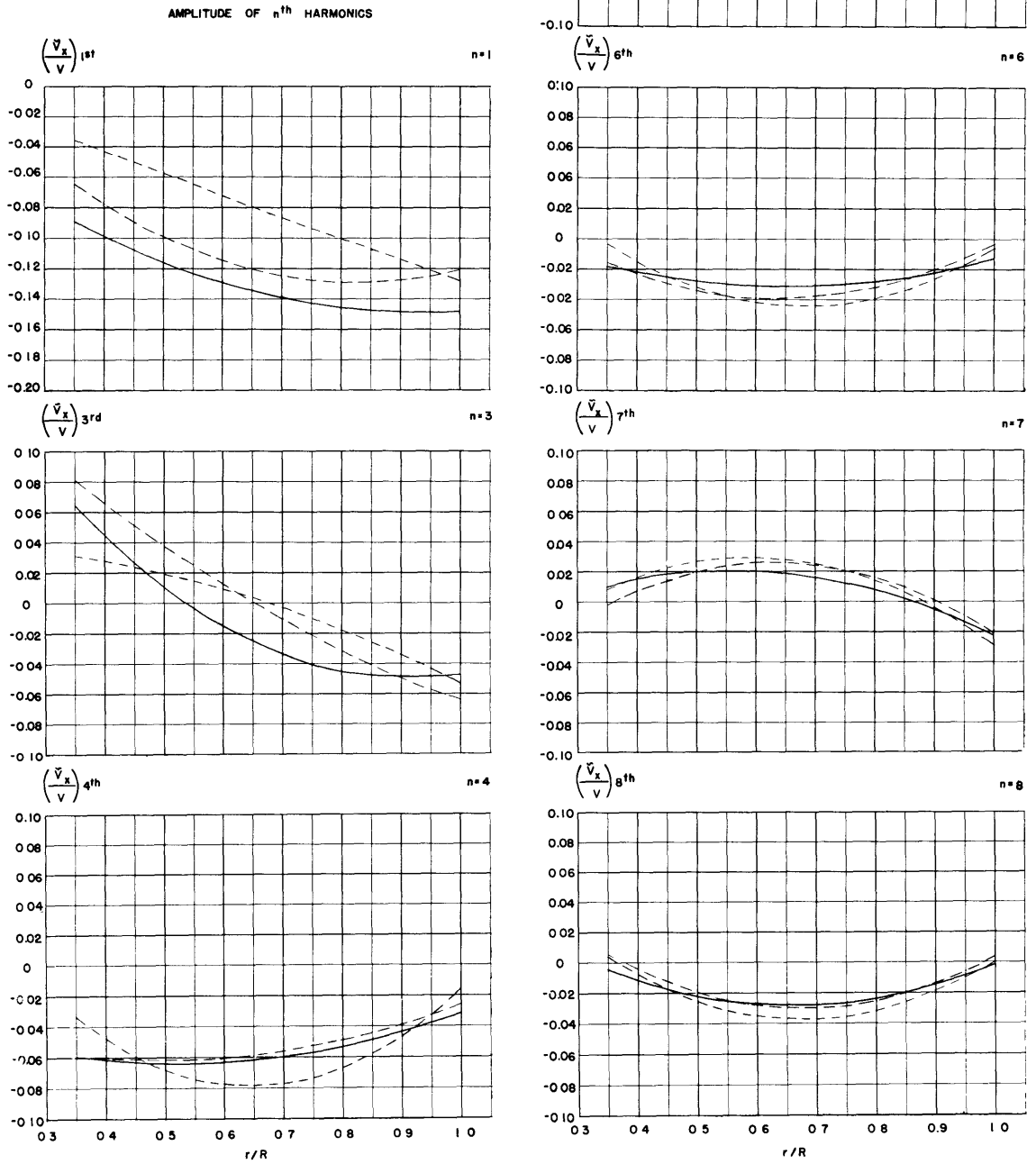| SYMBOL	TEST NUMBER	TUBE POSITION	RUDDER POSITION	SPEED (KNOTS)	DISPLACEMENT (POUNDS)	TRIM
——	3P	I	zero	4.38	2127	zero
- - -	5	I	B	4.38	2127	zero
——	6	I	A	4.38	2127	zero

AMPLITUDE OF nth HARMONICS
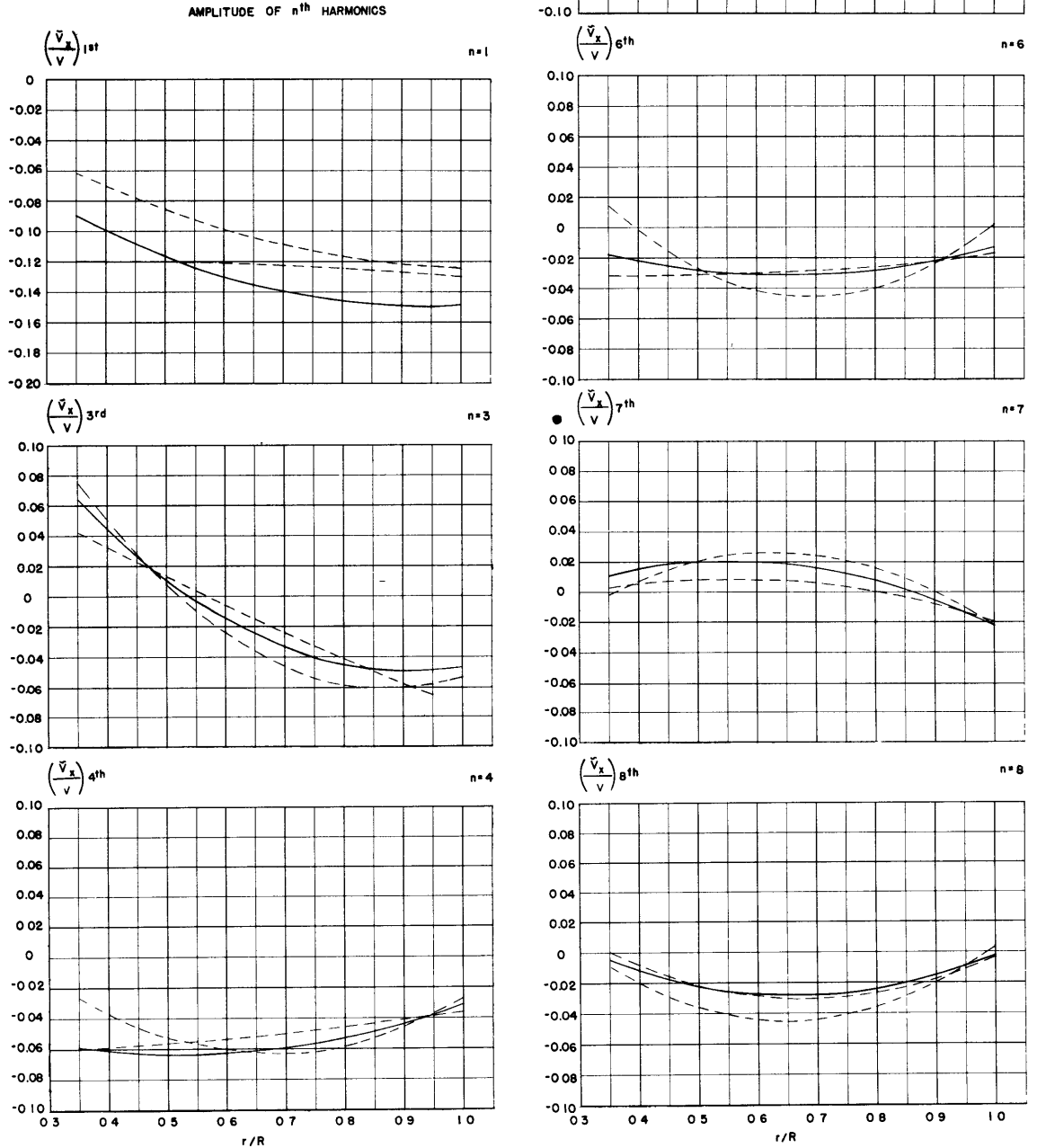

Figure 25 - Amplitudes of Harmonics of Longitudinal Velocity Components $(\widetilde{V}_x/V)$
Showing Differences Due to Variations in Longitudinal
Position of Rudder, Model 4210-5

$\left(\dfrac{\tilde{V}_x}{V}\right)_{5th}$ n = 5

SYMBOL	TEST NUMBER	TUBE POSITION	RUDDER POSITION	SPEED (KNOTS)	DISPLACEMENT (POUNDS)	TRIM
———	3P	1	none	4.38	2127	zero
— — —	7	2	none	438	2127	zero

AMPLITUDE OF nth HARMONICS

$\left(\dfrac{\tilde{V}_x}{V}\right)_{1st}$ n = 1

$\left(\dfrac{\tilde{V}_x}{V}\right)_{6th}$ n = 6

$\left(\dfrac{\tilde{V}_x}{V}\right)_{3rd}$ n = 3

$\left(\dfrac{\tilde{V}_x}{V}\right)_{7th}$ n = 7

$\left(\dfrac{\tilde{V}_x}{V}\right)_{4th}$ n = 4

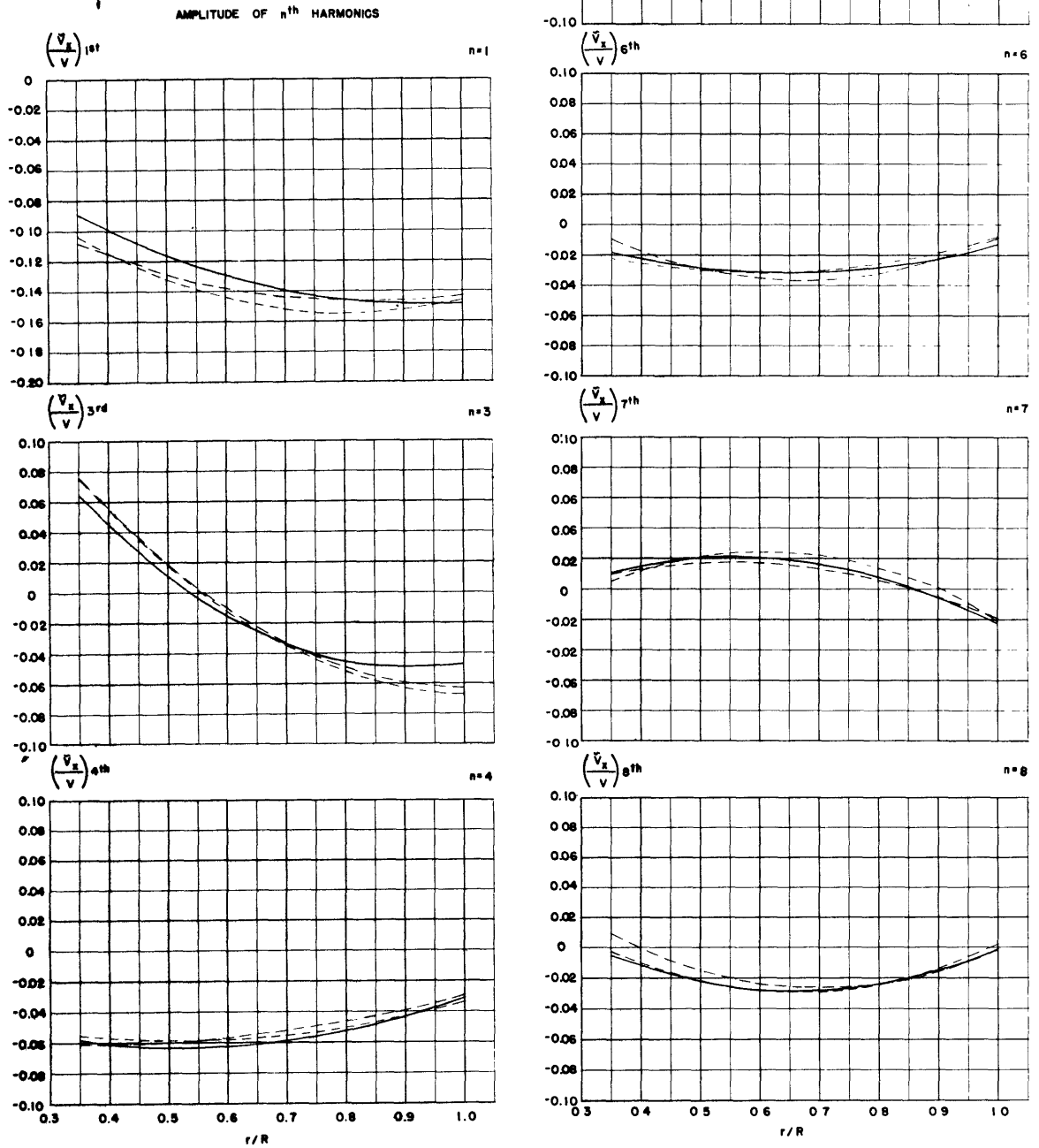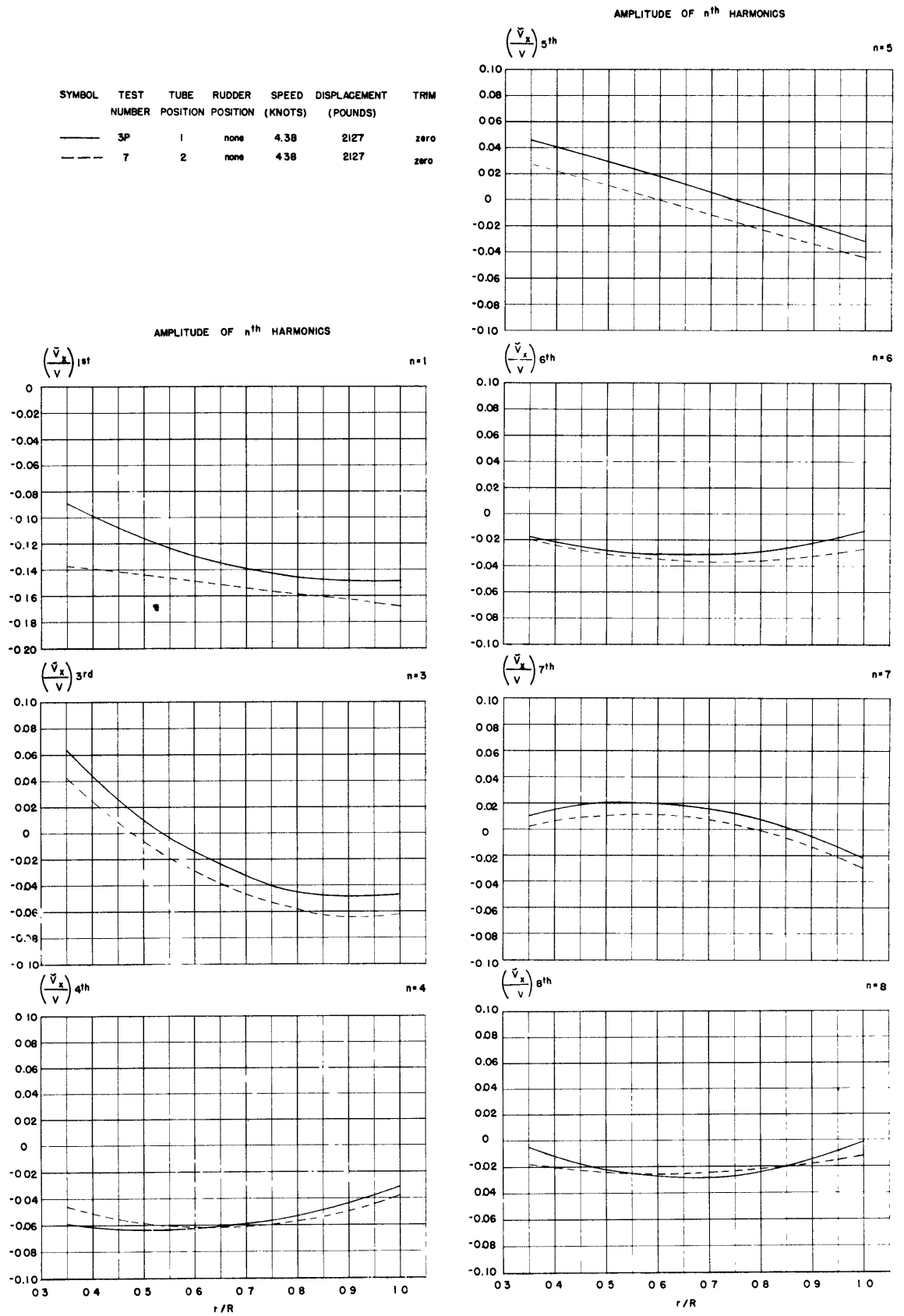$\left(\dfrac{\tilde{V}_x}{V}\right)_{8th}$ n = 8

r /R

r /R

Figure 26 - Amplitudes of Harmonics of Longitudinal Velocity Components $(\tilde{V}_x/V)$
Showing Differences Due to Variations in Longitudinal
Position of Plane of Survey, Model 4210-5

43

AMPLITUDE OF nth HARMONICS

$\left(\dfrac{\tilde{V}_x}{V}\right)_{5th}$ n = 5

SYMBOL	TEST NUMBER	TUBE POSITION	RUDDER POSITION	SPEED (KNOTS)	DISPLACEMENT (POUNDS)	TRIM (FEET)
——	3P	1	none	4.38	2127	zero
— — —	8	1	none	4.38	1276	0.48 x stern

AMPLITUDE OF nth HARMONICS

$\left(\dfrac{\tilde{V}_x}{V}\right)_{1st}$ n = 1

$\left(\dfrac{\tilde{V}_x}{V}\right)_{6th}$ n = 6

$\left(\dfrac{\tilde{V}_x}{V}\right)_{3rd}$ n = 3

$\left(\dfrac{\tilde{V}_x}{V}\right)_{7th}$ n = 7

$\left(\dfrac{\tilde{V}_x}{V}\right)_{4th}$ n = 4

$\left(\dfrac{\tilde{V}_x}{V}\right)_{8th}$ n = 8
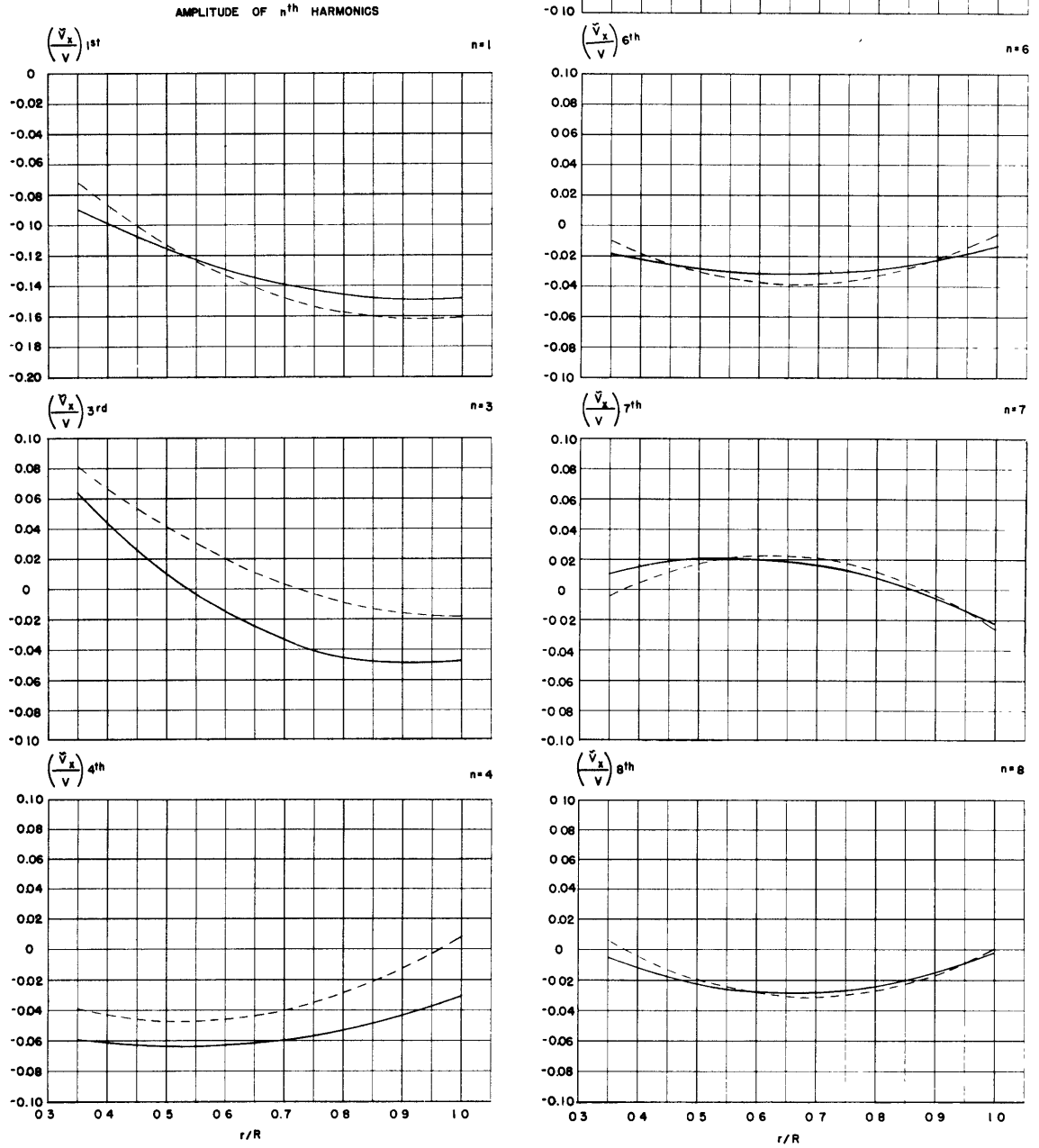
r/R

r/R

Figure 27 - Amplitudes of Harmonics of Longitudinal Velocity Components ($\tilde{V}_x/V$) Showing Differences Due to Variations in Displacement and Trim, Model 4210-5
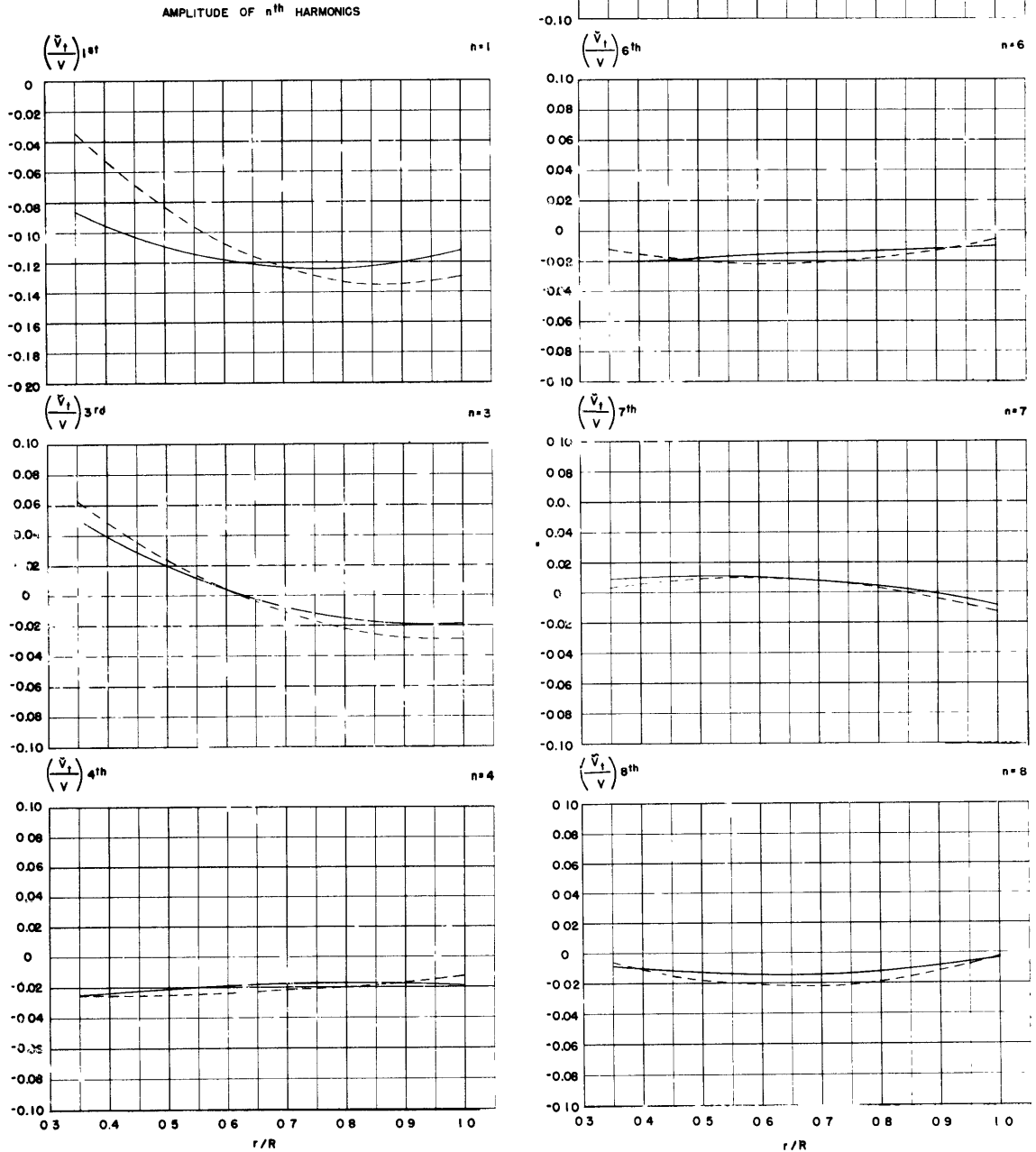
44

Figure 28 - Amplitudes of Harmonics of Tangential Velocity Components ($\tilde{V}_t/V$) Showing Differences Due to Variations in Longitudinal Position of Plane of Survey, Displacement, and Trim, Model 4210-5
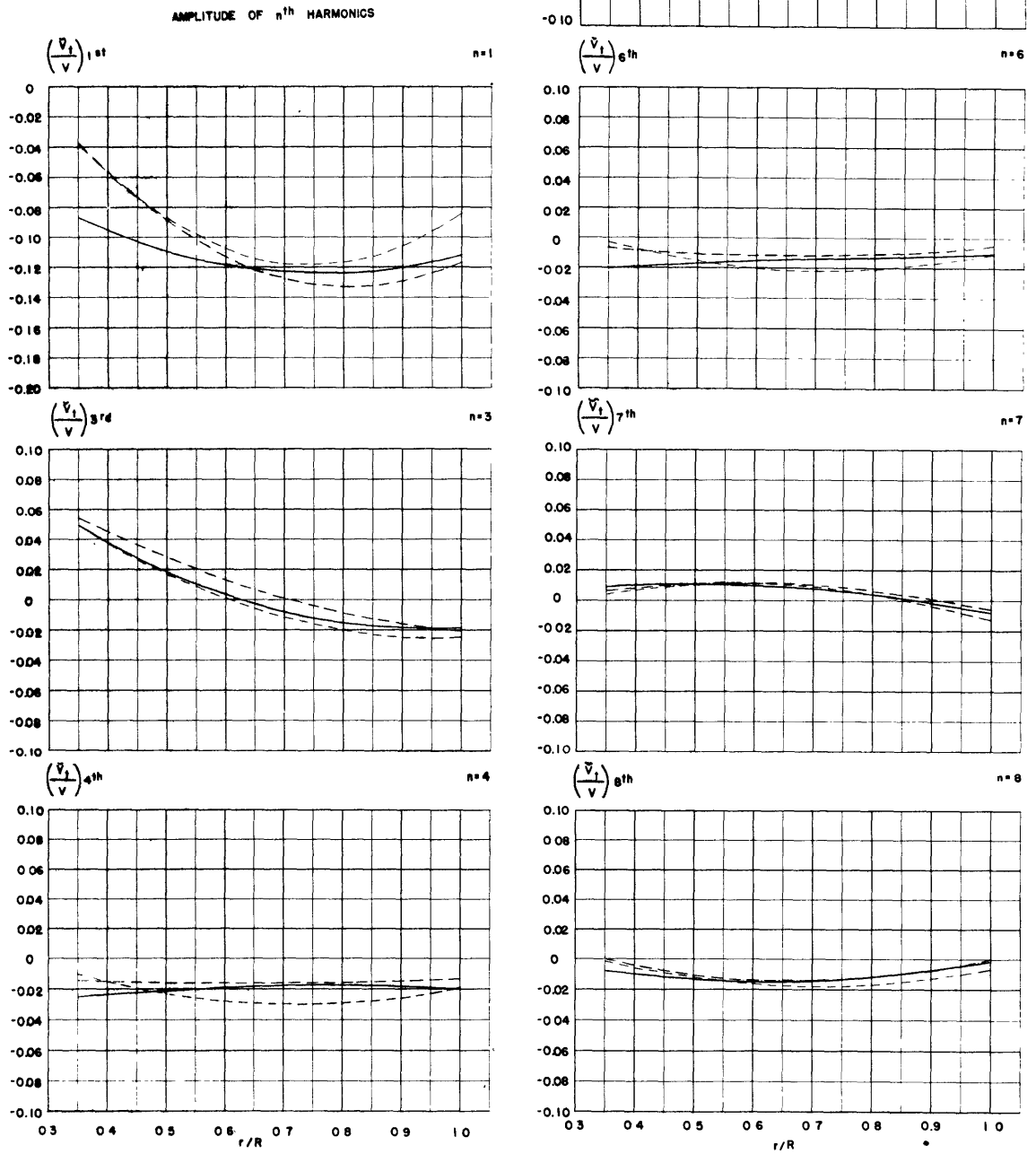
Figure 29 - Amplitudes of Harmonics of Tangential Velocity Components $(\tilde{V}_t/V)$ Showing Differences Due to Variations in Model Speed, Model 4210-5

AMPLITUDE OF nth HARMONICS

$\left(\dfrac{\tilde{V}_t}{V}\right)_{5^{th}}$ n = 5

SYMBOL	TEST NUMBER	TUBE POSITION	RUDDER POSITION	SPEED (KNOTS)	DISPLACEMENT (POUNDS)	TRIM
——	3P	I	none	4.38	2127	zero
— —	3PR	I	none	4.38	2127	zero
– – –	3S	I	none	4.38	2127	zero

AMPLITUDE OF nth HARMONICS

$\left(\dfrac{\tilde{V}_t}{V}\right)_{1^{st}}$ n = 1

$\left(\dfrac{\tilde{V}_t}{V}\right)_{3^{rd}}$ n = 3

$\left(\dfrac{\tilde{V}_t}{V}\right)_{4^{th}}$ n = 4

$\left(\dfrac{\tilde{V}_t}{V}\right)_{6^{th}}$ n = 6

$\left(\dfrac{\tilde{V}_t}{V}\right)_{7^{th}}$ n = 7

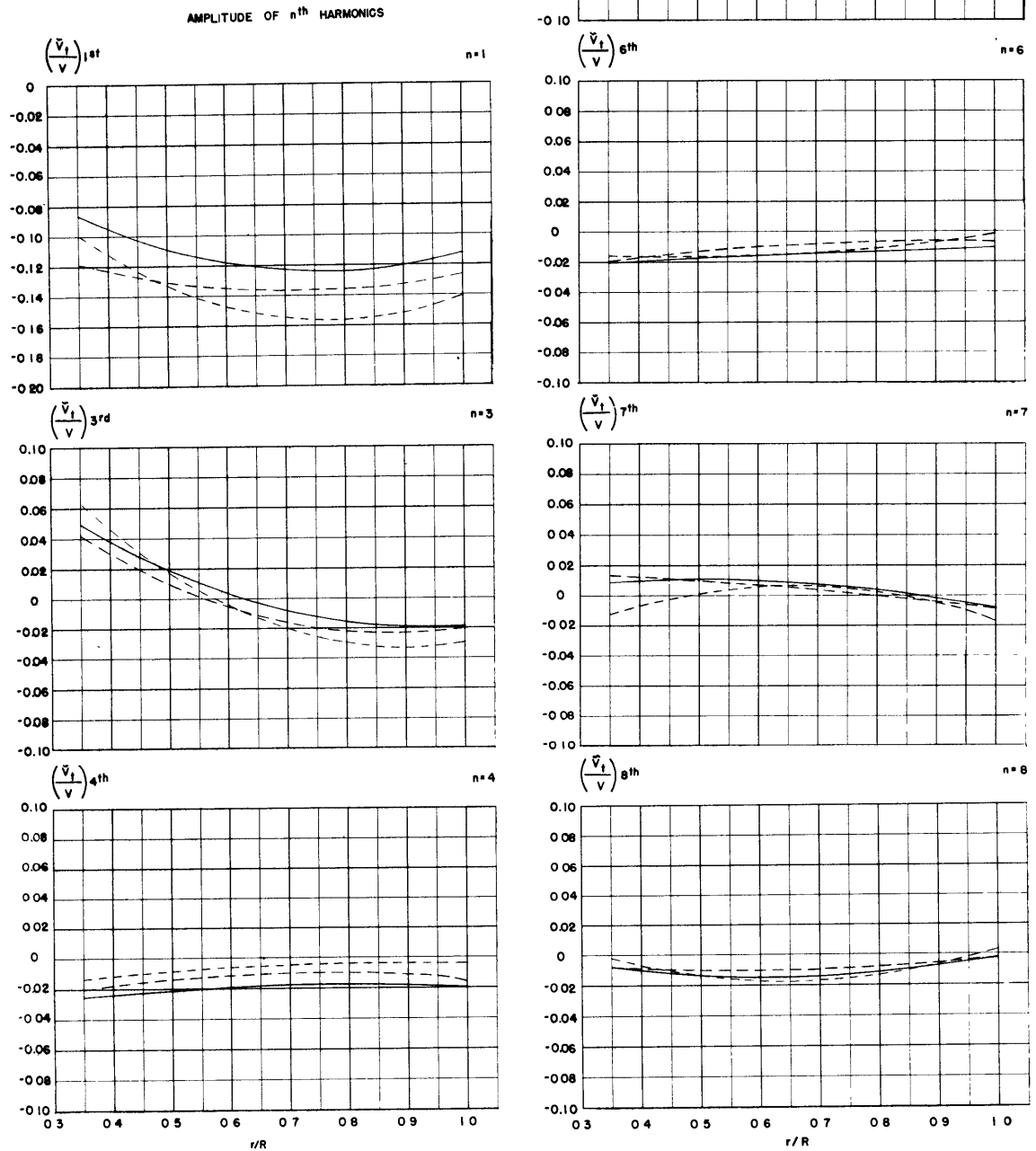$\left(\dfrac{\tilde{V}_t}{V}\right)_{8^{th}}$ n = 8

Figure 30 - Amplitudes of Harmonics of Tangential Velocity Components $(\tilde{V}_t/V)$ Showing Differences Due to Asymmetries and Repeatability, Model 4210-5

47

$\left(\dfrac{\tilde{V}_t}{V}\right)_{5^{th}}$ n = 5

0.10
0.08
0.06
0.04
0.02
0
-0.02
-0.04
-0.06
-0.08
-0.10

SYMBOL	TEST NUMBER	TUBE POSITION	RUDDER POSITION	SPEED (KNOTS)	DISPLACEMENT (POUNDS)	TRIM
———	3P	I	none	4.38	2127	zero
– – –	5	I	B	4.38	2127	zero
—·—·	6	I	A	4.38	2127	zero

AMPLITUDE OF nth HARMONICS

$\left(\dfrac{\tilde{V}_t}{V}\right)_{1^{st}}$ n = 1

0
-0.02
-0.04
-0.06
-0.08
-0.10
-0.12
-0.14
-0.16
-0.18
-0.20

$\left(\dfrac{\tilde{V}_t}{V}\right)_{6^{th}}$ n = 6

0.10
0.08
0.06
0.04
0.02
0
-0.02
-0.04
-0.06
-0.08
-0.10

$\left(\dfrac{\tilde{V}_t}{V}\right)_{3^{rd}}$ n = 3

0.10
0.08
0.06
0.04
0.02
0
-0.02
-0.04
-0.06
-0.08
-0.10

$\left(\dfrac{\tilde{V}_t}{V}\right)_{7^{th}}$ n = 7

0.10
0.08
0.06
0.04
0.02
0
-0.02
-0.04
-0.06
-0.08
-0.10

$\left(\dfrac{\tilde{V}_t}{V}\right)_{4^{th}}$ n = 4

0.10
0.08
0.06
0.04
0.02
0
-0.02
-0.04
-0.06
-0.08
-0.10

0.3 0.4 0.5 0.6 0.7 0.8 0.9 1.0

r/R

$\left(\dfrac{\tilde{V}_t}{V}\right)_{8^{th}}$ n = 8

0.10
0.08
0.06
0.04
0.02
0
-0.02
-0.04
-0.06
-0.08
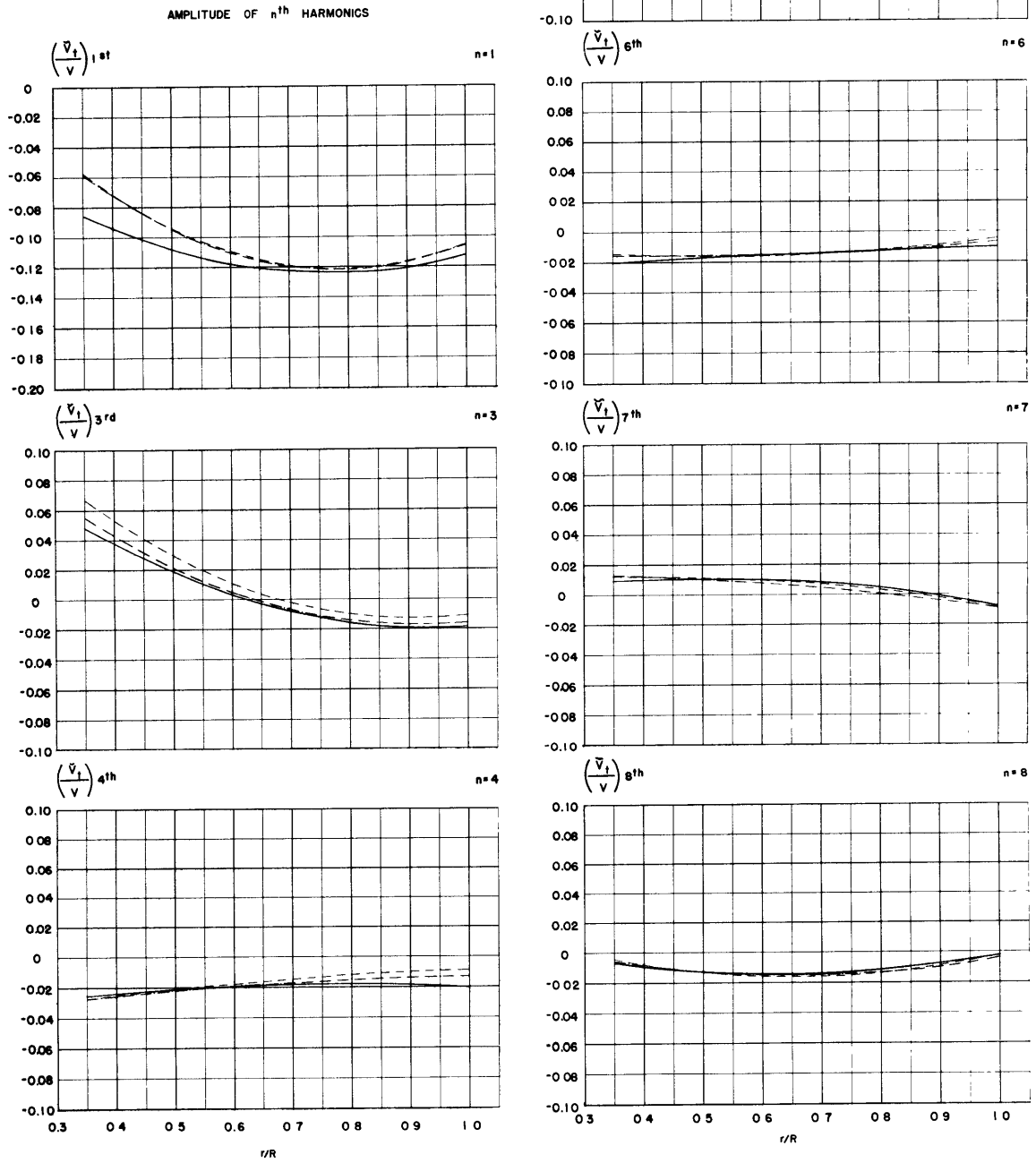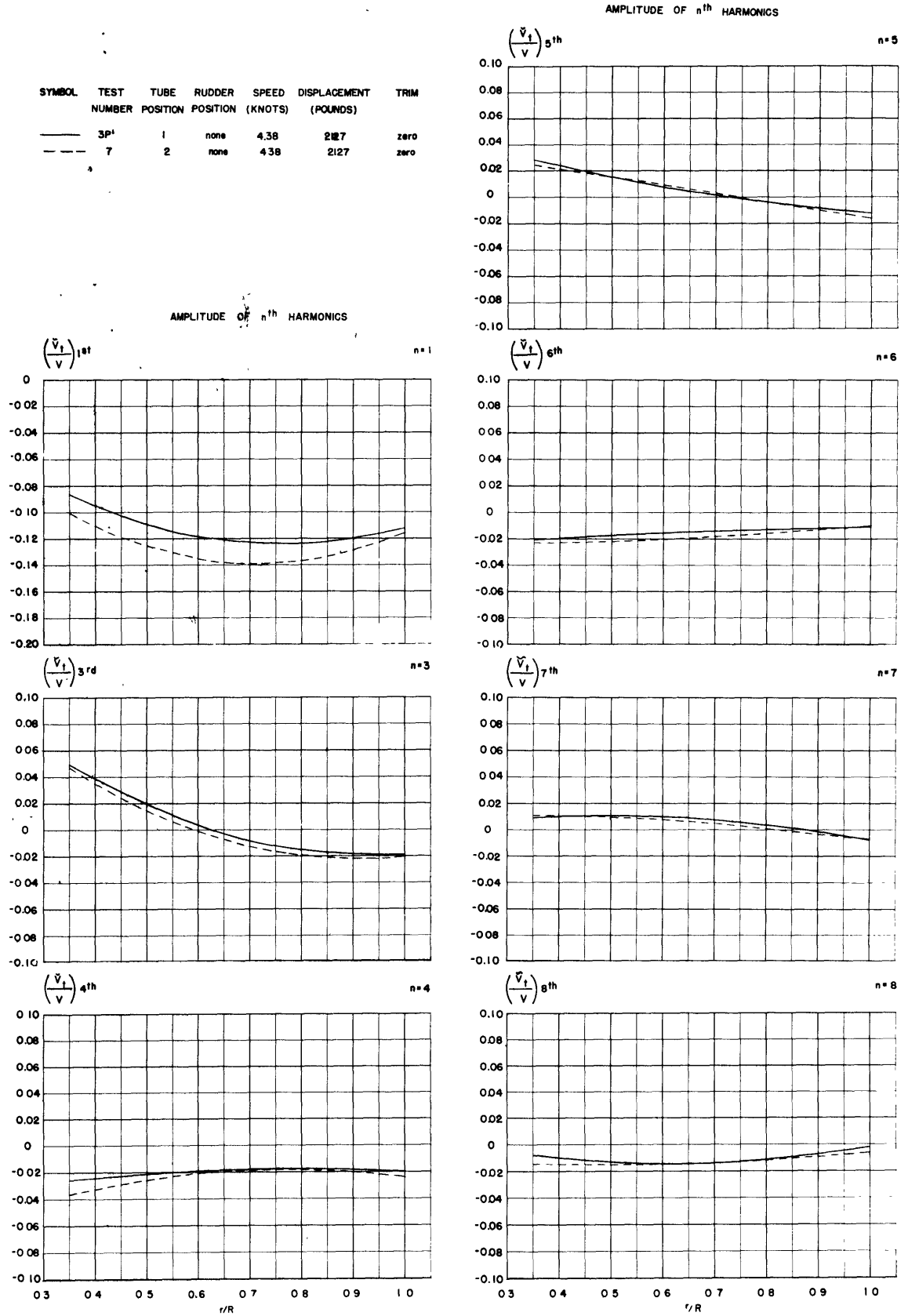-0.10

0.3 0.4 0.5 0.6 0.7 0.8 0.9 1.0

r/R
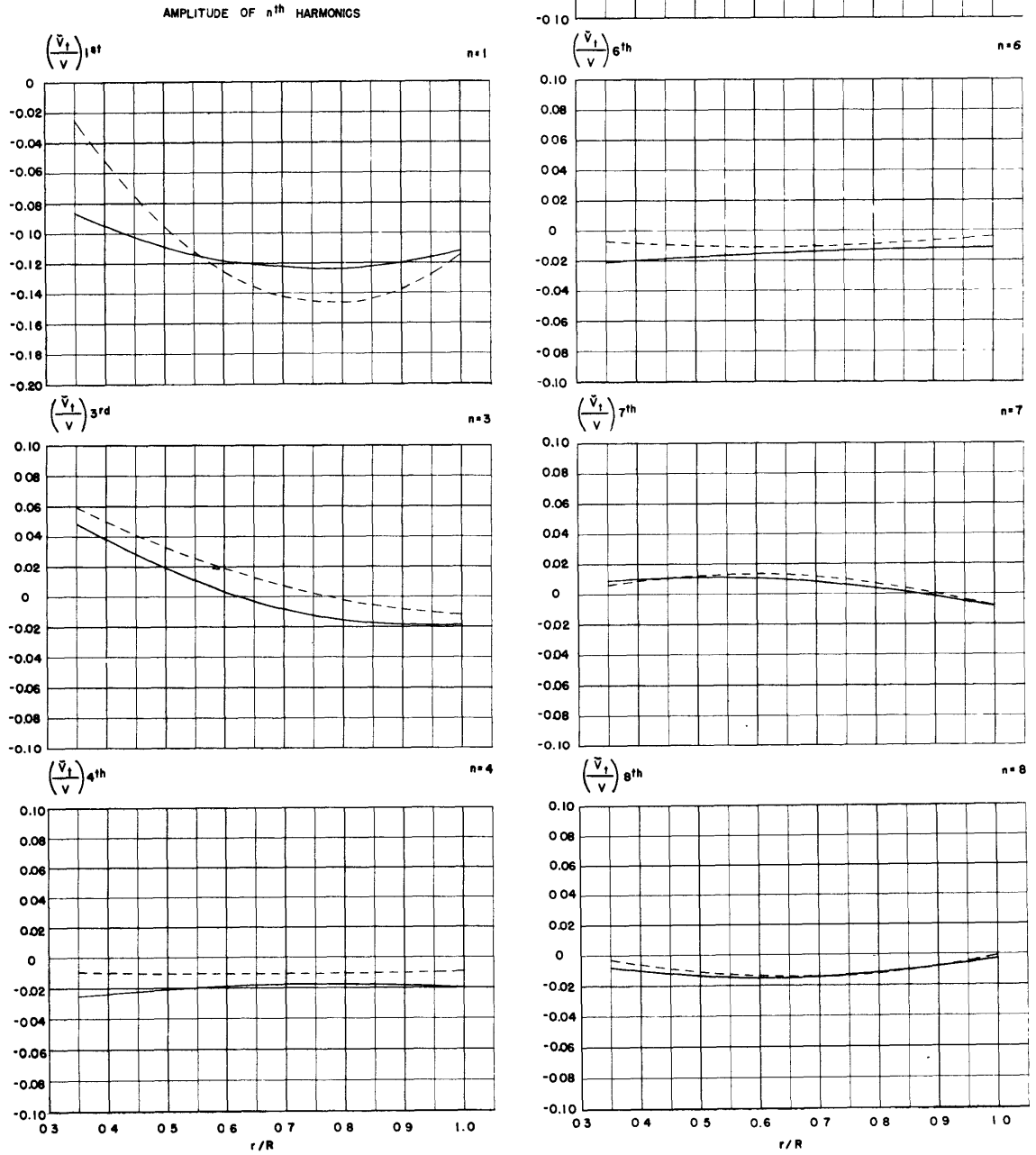
Figure 31 - Amplitudes of Harmonics of Tangential Velocity Components $(\tilde{V}_t/V)$ Showing Differences Due to Variations in Longitudinal Position of Rudder, Model 4210-5

48

AMPLITUDE OF nth HARMONICS

$\left(\dfrac{\tilde{V}_t}{V}\right)_{5^{th}}$ n = 5

SYMBOL	TEST NUMBER	TUBE POSITION	RUDDER POSITION	SPEED (KNOTS)	DISPLACEMENT (POUNDS)	TRIM
———	3P'	I	none	4.38	2127	zero
— — —	7	2	none	438	2127	zero

AMPLITUDE OF nth HARMONICS

$\left(\dfrac{\tilde{V}_t}{V}\right)_{1^{st}}$ n = 1

$\left(\dfrac{\tilde{V}_t}{V}\right)_{6^{th}}$ n = 6

$\left(\dfrac{\tilde{V}_t}{V}\right)_{3^{rd}}$ n = 3

$\left(\dfrac{\tilde{V}_t}{V}\right)_{7^{th}}$ n = 7

$\left(\dfrac{\tilde{V}_t}{V}\right)_{4^{th}}$ n = 4

$\left(\dfrac{\tilde{V}_t}{V}\right)_{8^{th}}$ n = 8

r/R

r/R

Figure 32 - Amplitudes of Harmonics of Tangential Velocity Components $(\tilde{V}_t/V)$
Showing Differences Due to Variations in Longitudinal
Position of Plane of Survey, Model 4210-5

Figure 33 - Amplitudes of Harmonics of Tangential Velocity Components $(\tilde{V}_t/V)$
Showing Differences Due to Variations in Displacement
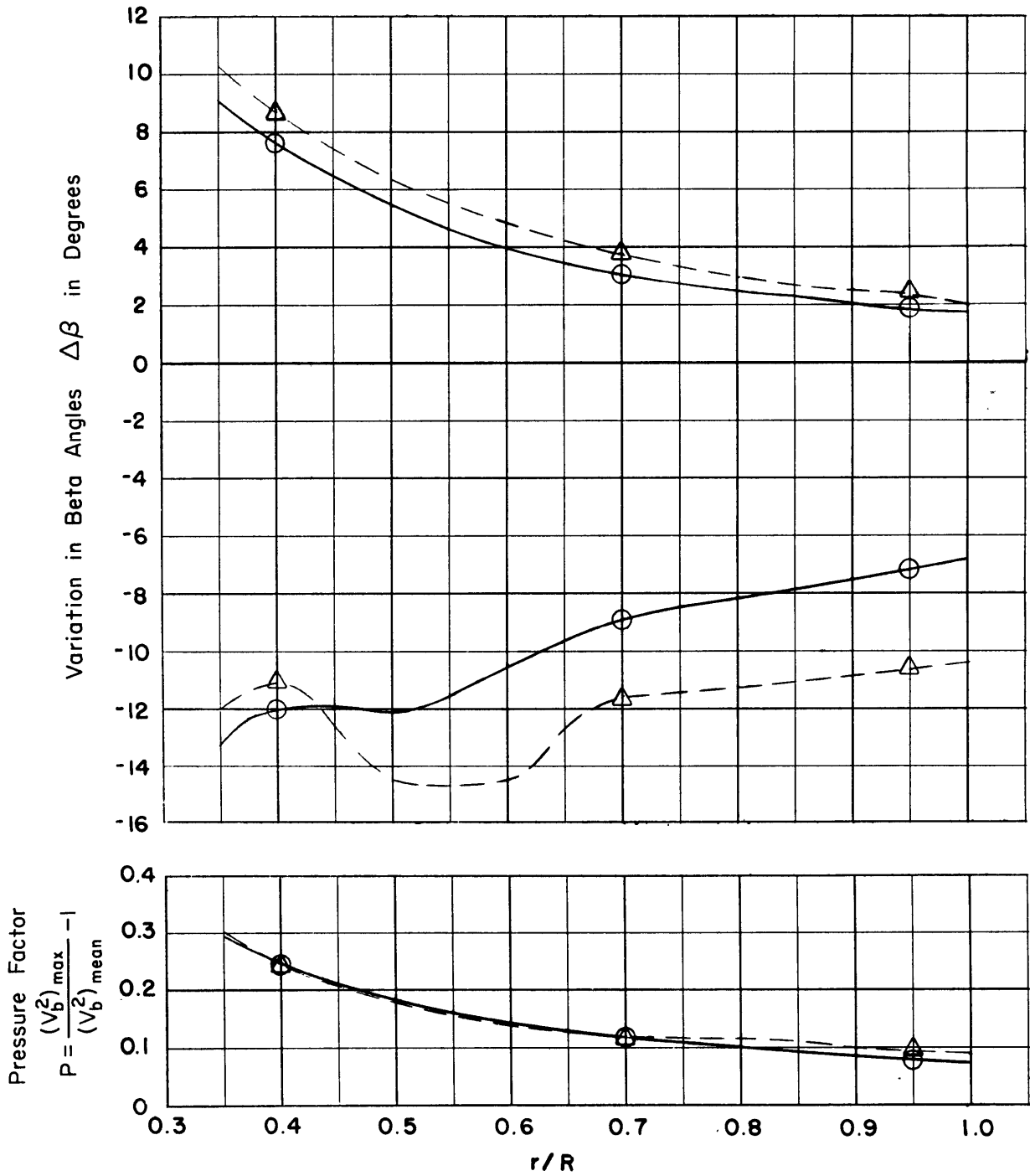and Trim, Model 4210-5

50
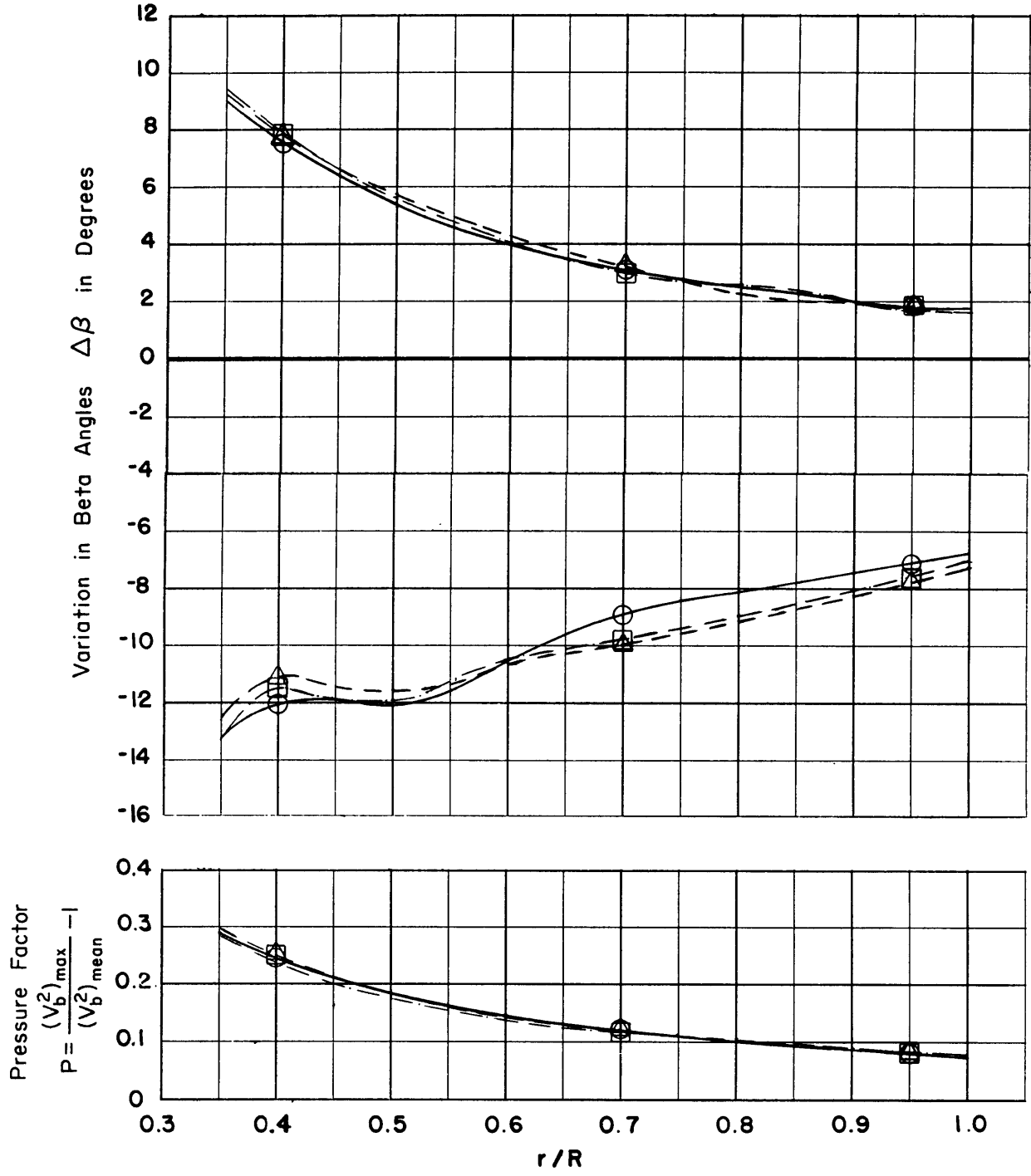
Figure 34 - Variations in Beta Angle ($\Delta \beta$) and Pressure Factor (P)
Due to Variations in Longitudinal Position of Plane of
Survey, Displacement, and Trim, Model 4210-5

51

Figure 35 - Variations in Beta Angle ($\triangle \beta$) and Pressure Factor (P)
Due to Variations in Model Speed, Model 4210-5

SYMBOL	TEST NUMBER	TUBE POSITION	RUDDER POSITION	SPEED (KNOTS)	DISPLACEMENT (POUNDS)	TRIM
—○—	3P	I	none	4.38	2127	zero
—□—	3PR	I	none	4.38	2127	zero
—△—	3S	I	none	4.38	2127	zero
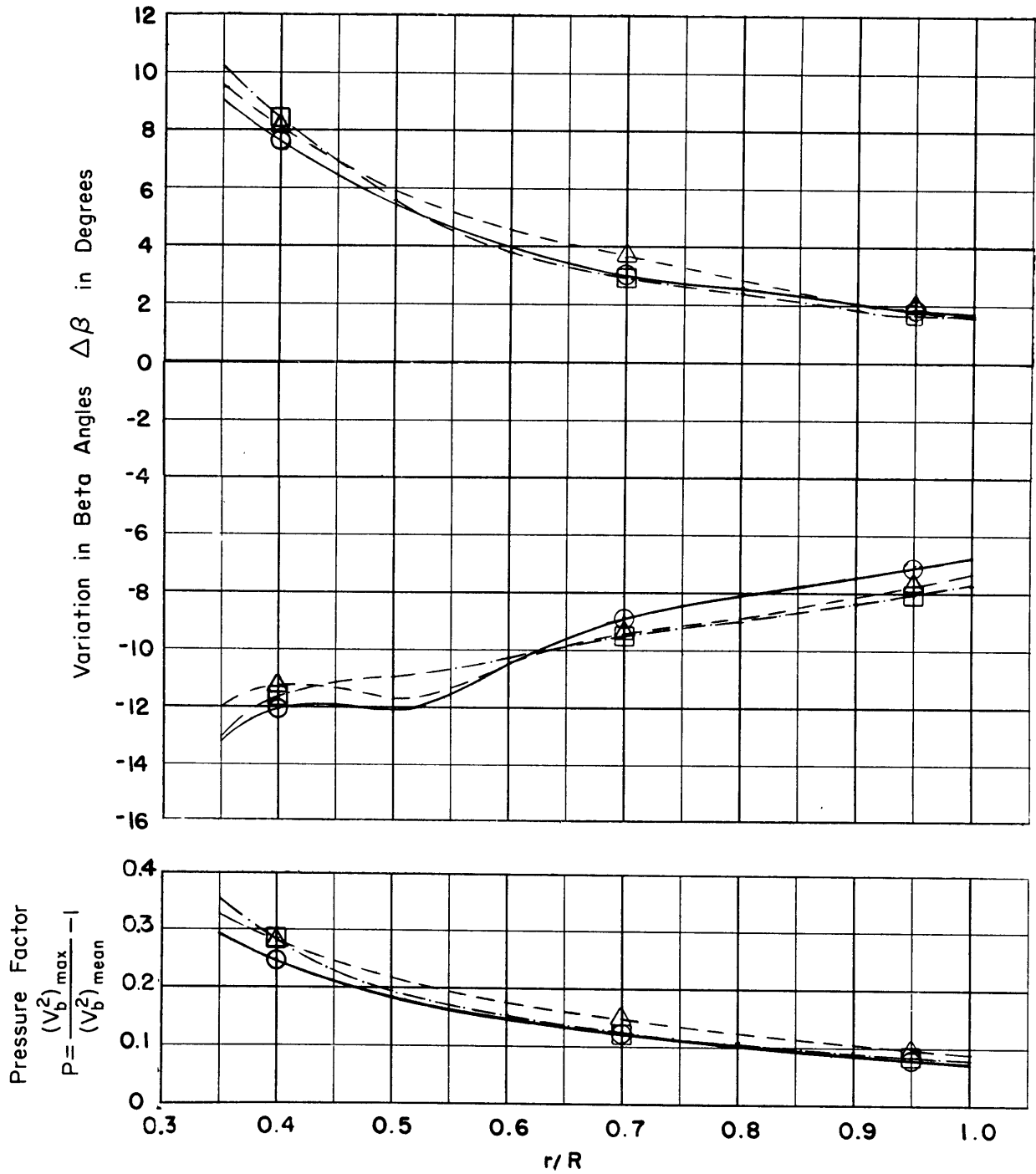
Figure 36 - Variations in Beta Angle ($\triangle \beta$) and Pressure Factor (P)
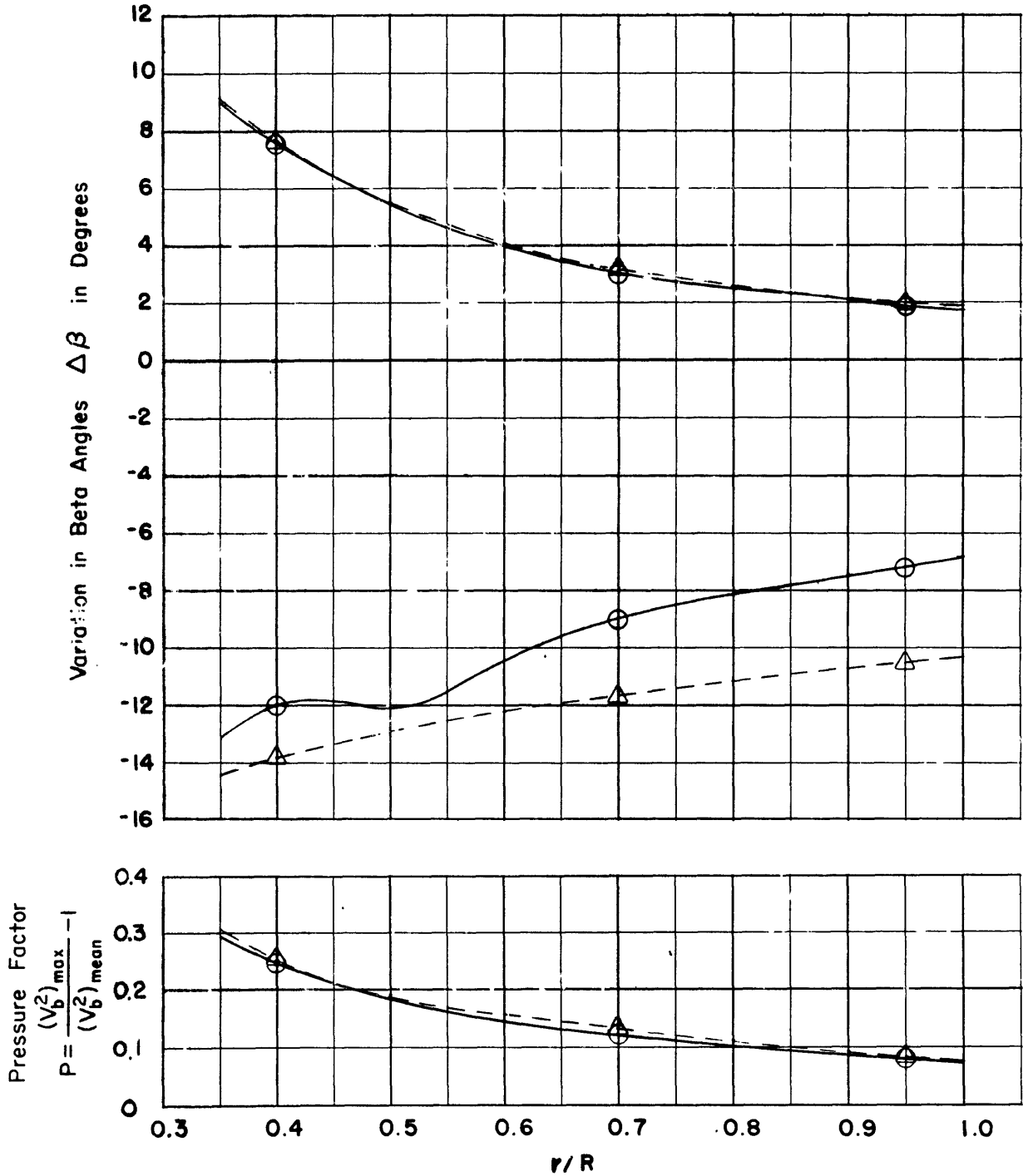Due to Asymmetries and Repeatability, Model 4210-5

Figure 37 - Variations in Beta Angle ($\Delta\beta$) and Pressure Factor (P)
Due to Variations in Longitudinal Position of Rudder,
Model 4210-5

SYMBOL	TEST NUMBER	TUBE POSITION	RUDDER POSITION	SPEED (KNOTS)	DISPLACEMENT (POUNDS)	TRIM
—O—	3P	1	none	4.38	2127	zero
—△—	7	2	none	4.38	2127	zero

Figure 38 - Variations in Beta Angle ($\Delta\beta$) and Pressure Factor (P) Due to Variations in Longitudinal Position of Plane of Survey, Model 4210-5

SYMBOL	TEST NUMBER	TUBE POSITION	RUDDER POSITION	SPEED (KNOTS)	DISPLACEMENT (POUNDS)	TRIM (FEET)
—⊖—	3P	I	none	4.38	2127	zero
—△—	8	I	none	4.38	1276	0.48 x stern
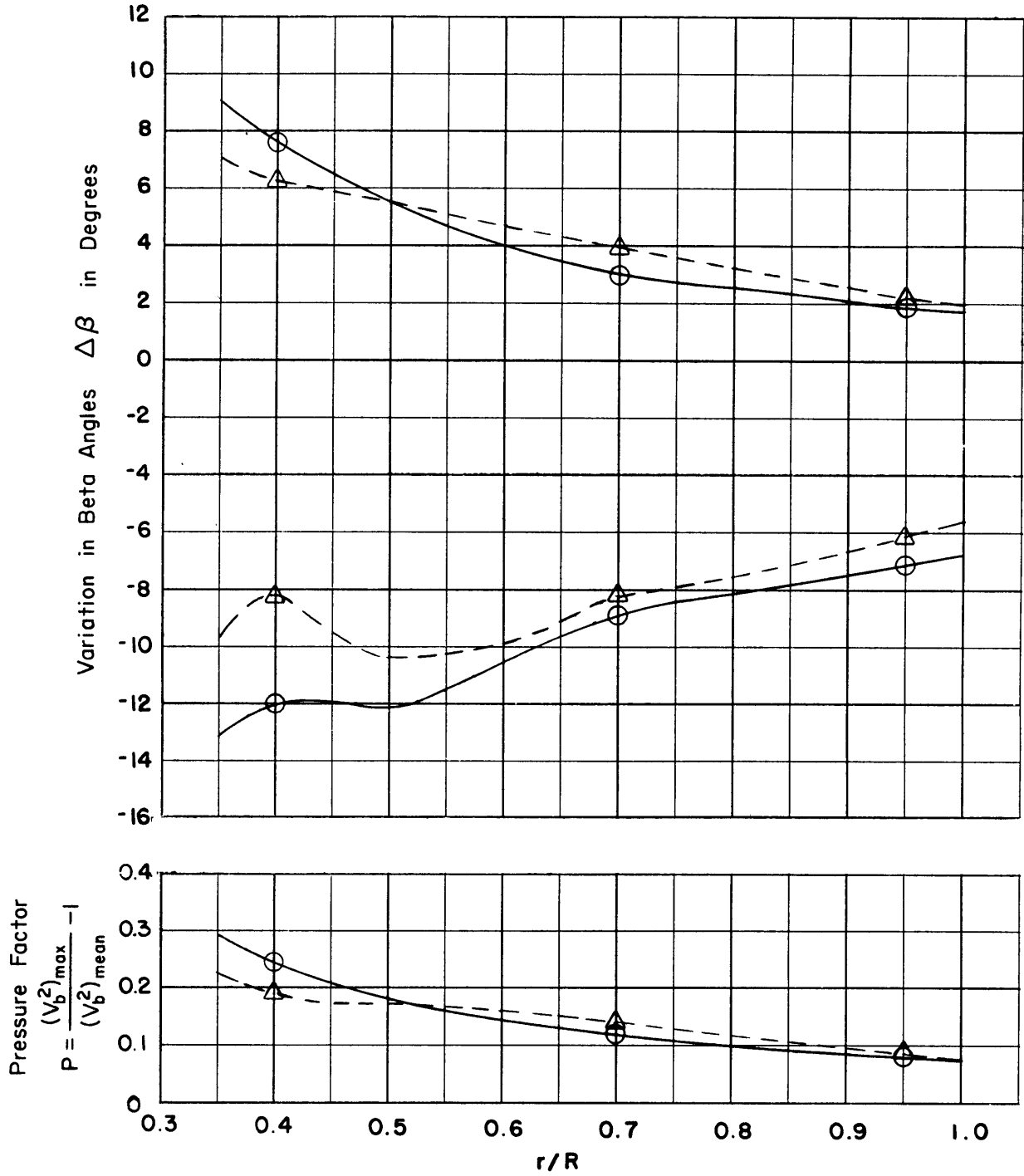
Figure 39 - Variations in Beta Angle ($\Delta\beta$) and Pressure Factor (P) Due to Variations in Displacement and Trim, Model 4210-5

n	A_n	B_n	C_n	ϕ_n	C_n/A_0
r/R = 0.3					
0	0.607709	0.	0.	0.	0.
1	-0.079313	-0.000000	0.079313	269.999905	0.130511
2	-0.236057	-0.000000	0.236057	269.999992	0.388438
3	0.085125	-0.000000	0.085125	90.000009	0.140076
4	-0.055836	-0.000000	0.055836	269.999985	0.091879
5	0.050932	-0.000000	0.050932	90.000013	0.083810
6	-0.013571	-0.000000	0.013571	269.999954	0.022331
7	0.005398	-0.000000	0.005398	90.000071	0.008882
8	0.002656	-0.000000	0.002656	90.000010	0.004371
9	-0.002773	-0.000000	0.002773	269.999977	0.004562
10	0.017034	-0.000000	0.017034	90.000027	0.028029
11	-0.005882	-0.000000	0.005882	269.999947	0.009678
12	0.018389	-0.000000	0.018389	90.000000	0.030260
13	-0.012220	-0.000000	0.012220	269.999973	0.020108
14	0.013593	-0.000000	0.013593	90.000022	0.022367
15	-0.013885	0.000000	0.013885	270.000000	0.022848
16	0.010850	0.000000	0.010850	89.999928	0.017853
r/R = 0.5					
0	0.729437	0.	0.	0.	0.
1	-0.116113	-0.000000	0.116113	269.999901	0.159182
2	-0.173883	-0.000000	0.173883	269.999989	0.238380
3	0.011468	-0.000000	0.011468	90.000123	0.015721
4	-0.063757	-0.000000	0.063757	269.999989	0.087406
5	0.028789	-0.000000	0.028789	90.000028	0.039467
6	-0.028508	-0.000000	0.028508	269.999981	0.039082
7	0.019749	-0.000000	0.019749	90.000022	0.027075
8	-0.021893	0.000000	0.021893	269.999996	0.030013
9	0.014912	-0.000000	0.014912	90.000031	0.020444
10	-0.013527	-0.000000	0.013527	269.999969	0.018544
11	0.014133	-0.000000	0.014133	90.000022	0.019375
12	-0.009671	0.000000	0.009671	270.000004	0.013259
13	0.011487	-0.000000	0.011487	90.000031	0.015748
14	-0.009724	-0.000000	0.009724	269.99997	0.013330
15	0.008721	0.000000	0.008721	89.999998	0.011956
16	-0.008998	0.000000	0.008998	270.000114	0.012336
r/R = 0.7					
0	0.795247	0.	0.	0.	0.
1	-0.139203	-0.000000	0.139203	269.999928	0.175043
2	-0.126563	-0.000000	0.126563	269.999966	0.159150
3	-0.033405	-0.000000	0.033405	269.999950	0.042006
4	-0.059734	-0.000000	0.059734	269.999989	0.075114
5	0.005305	-0.000000	0.005305	90.000161	0.006671
6	-0.031436	-0.000000	0.031436	269.999985	0.039530
7	-0.016225	-0.000000	0.016225	90.000023	0.020403
8	-0.027819	0.000000	0.027819	270.000008	0.034982
9	0.016067	-0.000000	0.016067	90.000021	0.020203
10	-0.022753	-0.000000	0.022753	269.999985	0.028612
11	0.017537	-0.000000	0.017537	90.000013	0.022052
12	-0.018178	0.000000	0.018178	270.000011	0.022858
13	0.017593	-0.000000	0.017593	90.000013	0.022123
14	-0.015918	-0.000000	0.015918	269.999992	0.020017
15	0.015625	0.000000	0.015625	89.999998	0.019648
16	-0.013757	0.000000	0.013757	270.000076	0.017299
r/R = 0.9					
0	0.805140	0.	0.	0.	0.
1	-0.148581	-0.000000	0.148581	269.999916	0.184540
2	-0.094099	-0.000000	0.094099	269.999958	0.116873
3	-0.049494	-0.000000	0.049494	269.999958	0.061472
4	-0.043766	-0.000000	0.043766	269.999977	0.054358
5	-0.019518	-0.000000	0.019518	269.999954	0.024242
6	-0.022355	-0.000000	0.022355	269.999977	0.027766
7	-0.005174	-0.000000	0.005174	269.999924	0.006427
8	-0.015123	0.000000	0.015123	270.000008	0.018783
9	0.000690	-0.000000	0.000690	90.000433	0.000857
10	-0.010646	-0.000000	0.010646	269.999977	0.013223
11	0.004331	-0.000000	0.004331	90.000039	0.005380
12	-0.007130	0.000000	0.007130	270.000023	0.008856
13	0.006099	-0.000000	0.006099	90.000024	0.007575
14	-0.004991	-0.000000	0.004991	269.999992	0.006199
15	0.006826	-0.000000	0.006826	90.000008	0.008478
16	-0.003427	0.000000	0.003427	270.000320	0.004256
r/R = 1.0					
0	0.789118	0.	0.	0.	0.
1	-0.148128	-0.000000	0.148128	269.999920	0.187714
2	-0.083437	-0.000000	0.083437	269.999947	0.105735
3	-0.046744	-0.000000	0.046744	269.999950	0.059235
4	-0.031302	-0.000000	0.031302	269.999958	0.039668
5	-0.032432	-0.000000	0.032432	269.999977	0.041100
6	-0.013311	-0.000000	0.013311	269.999962	0.016868
7	-0.022577	-0.000000	0.022577	269.999985	0.028611
8	-0.001792	0.000000	0.001792	270.000046	0.002271
9	-0.013197	-0.000000	0.013197	269.999992	0.016724
10	0.003407	-0.000000	0.003407	90.000028	0.004318
11	-0.008500	-0.000000	0.008500	269.999973	0.010772
12	0.005726	0.000000	0.005726	89.999978	0.007257
13	-0.006249	-0.000000	0.006249	269.999985	0.007919
14	0.006893	-0.000000	0.006893	90.000006	0.008735
15	-0.003461	-0.000000	0.003461	269.999992	0.004387
16	0.007396	0.000000	0.007396	89.999855	0.009373

THESE COLUMNS CAN BEST BE IDENTIFIED BY REFERRING TO THE FORM OF THE FOURIER EXPANSION

$$f(x) = A_0 + \sum_{n=1}^{\infty} C_n \sin (X_n + \phi_n)$$

WHERE $X_n = nx$, $C_n = \sqrt{A_n^2 + B_n^2}$, $\phi_n = \tan^{-1} \dfrac{A_n}{B_n}$ AND n IS THE ORDER OF THE HARMONIC.

Figure 40 - Tabulated Values of Harmonic Analysis for Longitudinal Component for Test 3P, Model 4210-5

n	A_n	B_n	C_n	ϕ_n

r/R = 0.3

n	A_n	B_n	C_n	ϕ_n
0	0.000000	0.	0.	0.
1	0.000000	-0.077183	0.077183	179.999996
2	-0.000000	-0.052806	0.052806	180.000017
3	-0.000000	0.061732	0.061732	359.999992
4	-0.000000	-0.027119	0.027119	180.000002
5	0.000000	0.032971	0.032971	0.000005
6	0.000000	-0.021661	0.021661	179.999996
7	-0.000000	0.007561	0.007561	359.999992
8	-0.000000	-0.005042	0.005042	180.000006
9	-0.000000	-0.000873	0.000873	180.000067
10	0.000000	0.006065	0.006065	0.000005
11	-0.000000	-0.004673	0.004673	179.999998
12	0.000000	0.007899	0.007899	0.000009
13	-0.000000	-0.006753	0.006753	179.999998
14	0.000000	0.005667	0.005667	0.000009
15	-0.000000	-0.006293	0.006293	180.000006
16	0.000000	0.003454	0.003454	0.000005

r/R = 0.5

n	A_n	B_n	C_n	ϕ_n
0	0.000000	0.	0.	0.
1	0.000000	-0.108803	0.108803	179.999996
2	-0.000000	-0.053606	0.053606	180.000011
3	-0.000000	0.019236	0.019236	359.999985
4	-0.000000	-0.020911	0.020911	180.000010
5	-0.000000	0.015395	0.015395	359.999992
6	-0.000000	-0.017558	0.017558	180.000006
7	0.000000	0.010808	0.010808	0.000001
8	-0.000000	-0.013530	0.013530	180.000004
9	0.000000	0.009061	0.009061	0.000003
10	-0.000000	-0.010161	0.010161	180.000006
11	0.000000	0.007412	0.007412	0.000002
12	-0.000000	-0.009317	0.009317	180.000006
13	0.000000	0.006886	0.006886	0.000002
14	-0.000000	-0.009167	0.009167	180.000006
15	0.000000	0.006702	0.006702	0.000004
16	-0.000000	-0.008686	0.008686	180.000004

r/R = 0.7

n	A_n	B_n	C_n	ϕ_n
0	0.000000	0.	0.	0.
1	0.000000	-0.123211	0.123211	179.999994
2	-0.000000	-0.053880	0.053880	180.000008
3	-0.000000	-0.007799	0.007799	180.000034
4	-0.000000	-0.017932	0.017932	180.000011
5	-0.000000	0.001382	0.001382	359.999924
6	-0.000000	-0.014311	0.014311	180.000011
7	-0.000000	0.007788	0.007788	359.999989
8	-0.000000	-0.014514	0.014514	180.000006
9	0.000000	0.009653	0.009653	0.000002
10	-0.000000	-0.014636	0.014636	180.000006
11	0.000000	0.009218	0.009218	0.000002
12	-0.000000	-0.014431	0.014431	180.000006
13	0.000000	0.009348	0.009348	0.000000
14	-0.000000	-0.013400	0.013400	180.000006
15	0.000000	0.009115	0.009115	0.000003
16	-0.000000	-0.011881	0.011881	180.000004

r/R = 0.9

n	A_n	B_n	C_n	ϕ_n
0	0.000000	0.	0.	0.
1	0.000000	-0.120404	0.120404	179.999992
2	-0.000000	-0.053629	0.053629	180.000006
3	-0.000000	-0.019371	0.019371	180.000015
4	-0.000000	-0.018181	0.018181	180.000011
5	-0.000000	-0.009069	0.009069	180.000017
6	-0.000000	-0.011919	0.011919	180.000013
7	-0.000000	-0.001500	0.001500	180.000057
8	-0.000000	-0.007995	0.007995	180.000011
9	-0.000000	0.000905	0.000905	359.999947
10	-0.000000	-0.007360	0.007360	180.000011
11	-0.000000	0.000745	0.000745	359.999958
12	-0.000000	-0.007445	0.007445	180.000006
13	-0.000000	0.000633	0.000633	359.999950
14	-0.000000	-0.007033	0.007033	180.000010
15	-0.000000	0.000945	0.000945	359.999973
16	-0.000000	-0.006130	0.006130	180.000008

r/R = 1.0

n	A_n	B_n	C_n	ϕ_n
0	0.000000	0.	0.	0.
1	0.000000	-0.112546	0.112546	179.999990
2	-0.000000	-0.053306	0.053306	180.000002
3	-0.000000	-0.019360	0.019360	180.000011
4	-0.000000	-0.019516	0.019516	180.000008
5	-0.000000	-0.012958	0.012958	180.000011
6	-0.000000	-0.011045	0.011045	180.000011
7	-0.000000	-0.008494	0.008494	180.000017
8	-0.000000	-0.001922	0.001922	180.000044
9	-0.000000	-0.006972	0.006972	180.000011
10	-0.000000	0.000683	0.000683	359.999935
11	-0.000000	-0.007346	0.007346	180.000010
12	-0.000000	0.000587	0.000587	359.999962
13	-0.000000	-0.007916	0.007916	180.000006
14	-0.000000	0.000125	0.000125	359.999817
15	-0.000000	-0.007108	0.007108	180.000008
16	-0.000000	0.000100	0.000100	359.999573

Figure 41 - Tabulated Values of Harmonic Analysis for Tangential
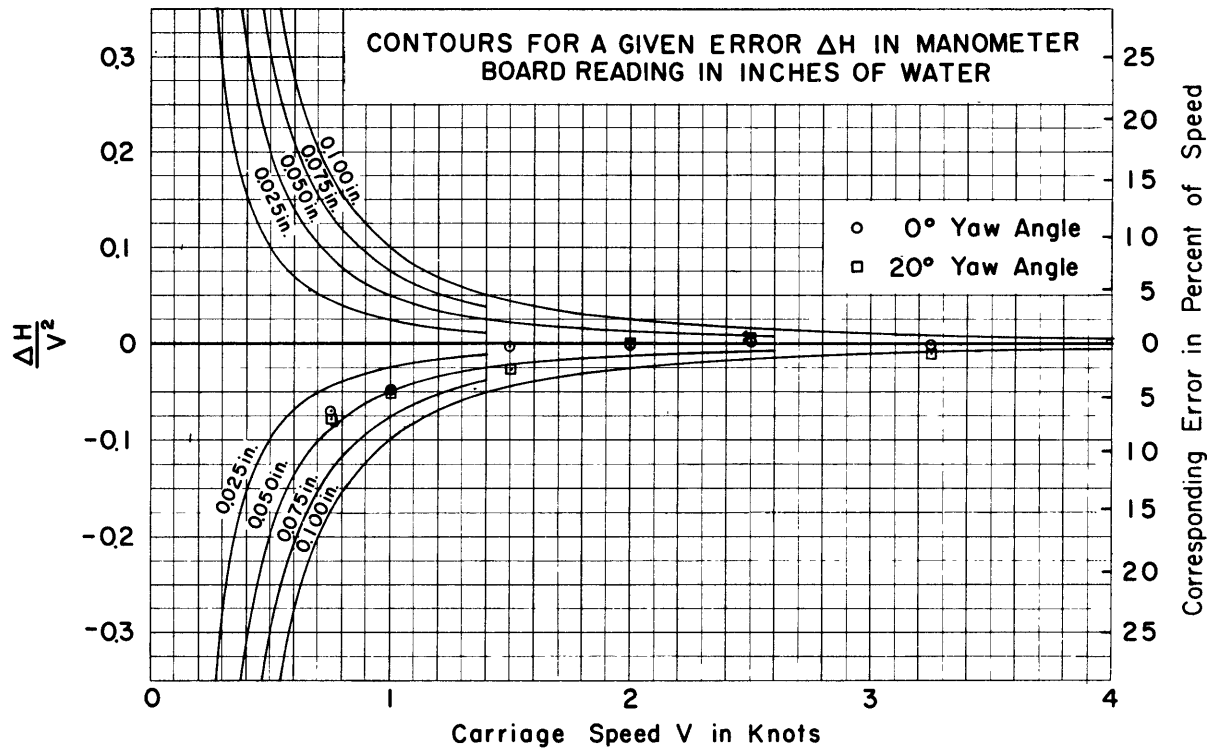Component for Test 3P, Model 4210-5
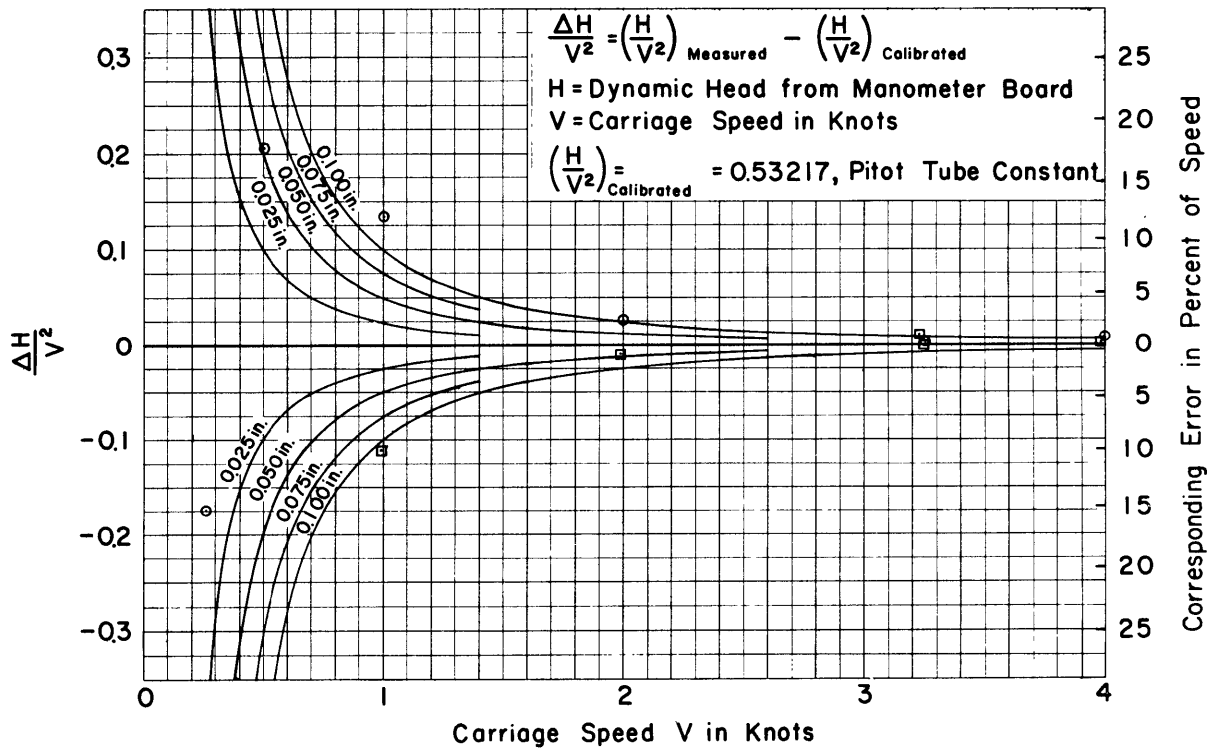
58

Figure 42a - 1-Inch 13-Hole Pitot Tube

Figure 42b - ½-Inch 5-Hole Pitot Tube

Figure 42 - Accuracy of Pitot Tube Measurements at Various Speeds

INITIAL DISTRIBUTION

Copies

13	CHBUSHIPS	
	3	Tech Lib (Code 210L)
	1	Appl Res (Code 340)
	1	Prelim Des (Code 420)
	1	Mach Sci & Res (Code 436)
	1	Hull Des (Code 440)
	1	Prop Shaft & Brng (Code 644)
	1	Lab Mgt (Code 320)
	1	Ship Silencing Br (Code 345)
	1	Cruisers and Destroyers Br (Code 523)
	2	Sci & Res (Code 442)
1	CHBUWEPS	
	1	Library (DLI-3)
3	CHONR	
	2	Fluid Dyn Br (Code 438)
	1	Library (Code 740)
1	SUPT, USNAVPGSCOL	
1	DIR, ORL	
1	ADMIN, MARAD	
20	DDC	
1	SNAME	
1	HD, NAME, MIT	
1	DIR, Iowa Inst. of Hydraulic Res	
1	DIR, St. Anthony Falls Hydraulic Lab	
1	HD, Dept NAME, Univ of Mich	
1	ADMIN, Inst NAVARCH, Webb	
1	DIR, Inst. of Eng Res, Univ of Calif	
1	DIR, Hydronautics, Inc.	
1	Bethlehem Steel Corporation, Shipbuilding Division	
1	Ingalls Shipbuilding Corporation	
1	Newport News Shipbuilding and Dry Dock Company	
1	Sun Shipbuilding and Dry Dock Co.	
1	Friede and Goldman, Inc.	
1	Gibbs and Cox	
1	George G. Sharpe Company	
1	Avondale Shipyards, Inc.	

DOCUMENT CONTROL DATA - R&D

(Security classification of title, body of abstract and indexing annotation must be entered when the overall report is classified)

1 ORIGINATING ACTIVITY *(Corporate author)*	2a. REPORT SECURITY CLASSIFICATION
David Taylor Model Basin	UNCLASSIFIED
	2b GROUP

3 REPORT TITLE

Wake Analysis of A Series 60, 0.60 Block Coefficient Model, Model 4210-5

4 DESCRIPTIVE NOTES *(Type of report and inclusive dates)*
Final

5 AUTHOR(S) *(Last name, first name, initial)*
Hadler, J.B.
Weaver, A.H.

6 REPORT DATE	7a. TOTAL NO. OF PAGES	7b. NO. OF REFS
October 1965	58	6

8a CONTRACT OR GRANT NO.	9a. ORIGINATOR'S REPORT NUMBER(S)
b PROJECT NO. S-R 009 01 01	TMB Report No. 2075
c Task 0103	9b. OTHER REPORT NO(S) *(Any other numbers that may be assigned this report)*
d	

10 AVAILABILITY/LIMITATION NOTICES

Distribution of this document is unlimited.

11 SUPPLEMENTARY NOTES	12. SPONSORING MILITARY ACTIVITY
	Bureau of Ships

13 ABSTRACT

This report presents the results of the wake analysis of a single-screw Series 60 model having a block coefficient of 0.60. The data presented include the interpolated longitudinal and tangential velocity distributions, and the effect on wake harmonics due to variations in speed, longitudinal position of rudder and plane of survey, draft, and trim.

DD FORM 1473
1 JAN 64

(ENCLOSURE 1)

14. KEY WORDS	LINK A		LINK B		LINK C	
	ROLE	WT	ROLE	WT	ROLE	WT

Wake Analysis
Series 60, 0.60 Block Coefficient Model (Model 4210-5)
High-Speed Cargo, Replenishment-Type Ship
    Effect of Rudder
    Effect of Speed
    Symmetry and Repeatability
    Plane of Measurement
    Trim and Displacement						

INSTRUCTIONS

1. ORIGINATING ACTIVITY: Enter the name and address of the contractor, subcontractor, grantee, Department of Defense activity or other organization (corporate author) issuing the report.

2a. REPORT SECURITY CLASSIFICATION: Enter the overall security classification of the report. Indicate whether "Restricted Data" is included. Marking is to be in accordance with appropriate security regulations.

2b. GROUP: Automatic downgrading is specified in DoD Directive 5200.10 and Armed Forces Industrial Manual. Enter the group number. Also, when applicable, show that optional markings have been used for Group 3 and Group 4 as authorized

3. REPORT TITLE: Enter the complete report title in all capital letters. Titles in all cases should be unclassified. If a meaningful title cannot be selected without classification, show title classification in all capitals in parenthesis immediately following the title.

4. DESCRIPTIVE NOTES: If appropriate, enter the type of report, e.g., interim, progress, summary, annual, or final. Give the inclusive dates when a specific reporting period is covered.

5. AUTHOR(S): Enter the name(s) of author(s) as shown on or in the report. Enter last name, first name, middle initial. If military, show rank and branch of service. The name of the principal author is an absolute minimum requirement.

6. REPORT DATE: Enter the date of the report as day, month, year, or month, year. If more than one date appears on the report, use date of publication.

7a TOTAL NUMBER OF PAGES: The total page count should follow normal pagination procedures, i.e., enter the number of pages containing information.

7b NUMBER OF REFERENCES. Enter the total number of references cited in the report.

8a CONTRACT OR GRANT NUMBER: If appropriate, enter the applicable number of the contract or grant under which the report was written.

8b, 8c, & 8d. PROJECT NUMBER: Enter the appropriate military department identification, such as project number, subproject number, system numbers, task number, etc.

9a. ORIGINATOR'S REPORT NUMBER(S): Enter the official report number by which the document will be identified and controlled by the originating activity. This number must be unique to this report.

9b OTHER REPORT NUMBER(S): If the report has been assigned any other report numbers (either by the originator or by the sponsor), also enter this number(s).

10. AVAILABILITY/LIMITATION NOTICES: Enter any limitations on further dissemination of the report, other than those imposed by security classification, using standard statements such as:

  (1) "Qualified requesters may obtain copies of this report from DDC."

  (2) "Foreign announcement and dissemination of this report by DDC is not authorized."

  (3) "U. S. Government agencies may obtain copies of this report directly from DDC. Other qualified DDC users shall request through

                                                                 ."

  (4) "U. S. military agencies may obtain copies of this report directly from DDC. Other qualified users shall request through

                                                                 ."

  (5) "All distribution of this report is controlled. Qualified DDC users shall request through

                                                                 ."

If the report has been furnished to the Office of Technical Services, Department of Commerce, for sale to the public, indicate this fact and enter the price, if known.

11. SUPPLEMENTARY NOTES: Use for additional explanatory notes.

12. SPONSORING MILITARY ACTIVITY: Enter the name of the departmental project office or laboratory sponsoring (paying for) the research and development. Include address.

13. ABSTRACT: Enter an abstract giving a brief and factual summary of the document indicative of the report, even though it may also appear elsewhere in the body of the technical report. If additional space is required, a continuation sheet shall be attached.

It is highly desirable that the abstract of classified reports be unclassified. Each paragraph of the abstract shall end with an indication of the military security classification of the information in the paragraph, represented as (TS), (S), (C), or (U).

There is no limitation on the length of the abstract. However, the suggested length is from 150 to 225 words.

14. KEY WORDS: Key words are technically meaningful terms or short phrases that characterize a report and may be used as index entries for cataloging the report. Key words must be selected so that no security classification is required. Identifiers, such as equipment model designation, trade name, military project code name, geographic location, may be used as key words but will be followed by an indication of technical context. The assignment of links, roles, and weights is optional.

David Taylor Model Basin. Report 2075.
WAKE ANALYSIS OF A SERIES 60, 0.60 BLOCK COEFFI-
CIENT MODE, MODEL 4210-5, by J.B. Hadler and A.H. Weaver.
Oct 1965. viii, 60p. illus., graphs, diags., tabs., refs.
UNCLASSIFIED

This report presents the results of the wake analysis of a
single-screw Series 60 model having a block coefficient of 0.60.
The data presented include the interpolated longitudinal and
tangential velocity distributions, and the effect on wake harmon-
ics due to variations in speed, longitudinal position of rudder
and plane of survey, draft, and trim.

1. Wakes--Analyses--Speed
   effects
2. Wakes--Analyses--Rudder
   effects
3. Wakes--Analyses--Plane
   of measurement effects
4. Wakes--Analyses--Draft
   effects
5. Wakes--Analyses--Trim
   effects
6. Fast replenishment ships--
   Wakes--Model tests
7. Ship models--Model TMB
   series 60--0.60 block
   coefficient
8. Ship models--Model TMB
   4210-5
I. Hadler, Jacques B.
II. Weaver, Albert H.